DOE/SF/18852--TLD

Cassini RTG Program CDRL Transmittal

TO:
U.S. Department of Energy
6633 Canoga Avenue
Canoga Park, California 91303
Attention: K. Vijaiyan
Project Manager

DISTRIBUTION:

Symbol	Copies
A	5
B	1
C	1
D	1
E	2
H	2
J	20
K	1

Cassini RTG Program
Contract No: DE-AC03-91SF18852

In Reply Refer to: **CON #1481**
Date: **24 February 1996**

CDRL Number: **Reporting Requirement 4.F (Document No. RR16)**

Title: **Monthly Technical Progress Report (1 January 1996 through 28 January 1996)**

Approval Requirements:

Approval [ ] None [X]

Contract Period: **11 January 1991 through 30 April 1998**

INTRODUCTION

The technical progress achieved during the period 1 January 1996 though 28 January 1996 on Contract DE-AC03-91SF18852 Radioisotope Thermoelectric Generators and Ancillary Activities is described herein.

This report is organized by program task structure.

- 1.X Spacecraft Integration and Liaison
- 2.X Engineering Support
- 3.X Safety
- 4.X Qualified Unicouple Production
- 5.X ETG Fabrication, Assembly, and Test
- 6.X Ground Support Equipment (GSE)
- 7.X RTG Shipping and Launch Support
- 8.X Designs, Reviews, and Mission Applications
- 9.X Project Management, Quality Assurance, Reliability, Contract Changes, CAGO Acquisition (Operating Funds), and CAGO Maintenance and Repair
- H.X CAGO Acquisition (Capital Funds)

Note: Task H.X scope is included in SOW ¶ Task 9.5.
Task H. was created to manage CAGO acquired with capital equipment funding.

Approved: R. J. Hemler, Manager
Space Power Programs

Internal Distribution:
Technical Report List

From: Lockheed Martin Missiles & Space
Room 10B50 Building B
720 Vandenberg Road
King of Prussia, PA 19406

Signature:
Joseph M. Waks
Contracts Manager

MASTER

Monthly Technical Report
Progress by Major Task

TASK 1 SPACECRAFT INTEGRATION AND LIAISON

Preparations for the JPL requested capacitance test on the E-7 converter are continuing. The test cable assembly was provided to JPL for measurements and subsequently returned. Performance of the capacitance test is scheduled next month in conjunction with vacuum processing of E-7 at Lockheed Martin.

TASK 2 ENGINEERING SUPPORT

Specifications/Drawings

ECNs for the ETG/RTG activities were prepared and processed through CCB approval. The GPHS-RTG Product Specification for Cassini (23009148) was approved and issued under CDRL B.1.

RTG Fuel Form, Fueling, and Test Support/Liaison

Work continued, as necessary, on the evaluation and disposition of fuel processing related non-conformance reports from LANL. In a related task, possible revisions to the compositional requirements for the LANL fuel powder, pellet, and fueled clad specifications were evaluated. Available information on fuel impurities is being gathered by a number of organizations to determine the justification for possible revisions.

Lockheed Martin personnel, working at Mound, installed the F-2 PRD adapter plate, performed the PRD fit check, installed the RTD harness and connector bracket, and performed RTD harness electrical measurements. All measurements were satisfactory. In addition, minor scratches and surface imperfections on the exterior of the generator were touched up with PD 224 paint.

TASK 3 SAFETY ANALYSIS TASK

The safety analysis task is comprised of four major activities: 1) Launch Accident Analysis; 2) Reentry Analysis; 3) Consequence and Risk Analysis and 4) the Safety Test Program. An overview of the significant issues related to this task for this period, followed by details in each of the four major activities, is provided in the following subsections.

A listing of the INSRP meetings held through January 1996 is provided in Table 3-1.

Table 3-1. Safety Analysis Task – Completed INSRP Reviews

Date	*Review*
14 February 1995	INSRP PSAR Review
20 April 1995	PSSP Review of LASEP-T Status
27 April 1995	RESP Review of Reentry CFD and Thermal Analysis
3 May 1995	MET Review of SPARRC Status
16 May 1995	BEES Review of SPARRC Status
8 June 1995	Working Meeting with INSRP on Launch Accident Analysis Treatment of Variability and Uncertainty
10 August 1995	RESP Review of Reentry CFD and Thermal Analysis
23 August 1995	LASP Review of PSAR Comments and Databook Items
24 August 1995	INSRP Review of Launch Accident Analysis Treatment of Variability and Uncertainty
19 September 1995	Review Meeting with INSRP MET Chairperson
28 September 1995	Working Meeting with INSRP on Reentry Analysis Treatment of Variability and Uncertainty
25-27 October 1995	INSRP PSSP Review of LASEP-T and RESP Review of Reentry
6-8 November 1995	MET and BEES Review of SPARRC Status
29-30 November 1995	INSRP Safety Analysis and Status Review
17-19 January 1996	INSRP Review of LASEP-T and Out-of-Orbit Preliminary Analysis Results

Launch Accident Analysis

Principal activities during this reporting period included the issuance of LASEP-T Rev. 1.0, generation of source terms for case 1.9 (Centaur explosion), review of preliminary source term and consequence results from case 1.9 with INSRP, and completion of PIRs documenting LASEP-T Rev. 1.0 subroutines.

As a result of previous INSRP and internal reviews, several areas of excess conservatism had been identified in LASEP-T Rev. 0.0, including RTG side-on blast wave effects on fueled clad distortions and the relationship between fueled clad distortion and fuel release. Modifications to LASEP-T subroutines were completed this month. They included incorporating blast wave flow-around effects for RTG side-on fueled clad distortions into the SVIMPT subroutine. They also included replacing the continuous representation of fuel release vs. fueled clad distortion percentage in the DST2REL subroutine with a bimodal behavior depicting small (hook) and large (punch-through) release types consistent with visual inspection of BCI and SVT test hardware. In addition to these changes, LASEP-T Rev. 1.0 includes a vaporization subroutine to treat the influence of a liquid propellant fireball on plutonia particle size distributions. This model is updated from that used in the Galileo and Ulysses FSARs and now includes convective heat transfer and sublimation heat loss effects for plutonia particles.

LASEP-T Rev. 1.0 was utilized to generate preliminary source terms for eleven phase 0 and phase 1 composite accident cases, representing both pre and post lift-off accident scenarios. Insults to fueled clads were tracked and categorized with releases further categorized by location and coincidence with liquid propellant fireballs.

Results from a single representative case (1.9 - Centaur explosion) were provided to the SPARRC consequence model to demonstrate interface fidelity prior to the generation of results for the draft FSAR. As described later, consequence was calculated for the average case 1.9 release for each of 128 weather days from a five year October database.

Results of the LASEP-T Rev. 1.0 source term generation and consequence analysis described above were reviewed with INSRP in Valley Forge, PA, on 17-19 January. Representatives of the Power Systems, Launch Accident, Meteorology and Biological Effects subpanels attended the review which served as the second part of the Updated Safety Analysis Review.

Design reports (PIRs) describing the operation, assumptions, and source listings of the LASEP-T Rev. 1.0 subroutines were completed in late January. These documents were undergoing internal review at the end of the month and are expected to be issued for distribution to INSRP in mid-February.

Sandia National Labs (SNL) is continuing to develop a "state-of-the-art" plutonia vaporization model and agglomeration model to be completed in late March. Comparative studies with the LASEP-T vaporization model are planned following delivery of the completed model. Status of this activity was reviewed at SNL in early January by members of both LMMS and Foils Engineering. The SNL model will be modified to accept time dependent introduction of liquid propellant reactants to a fireball consistent with on-going hydrocode simulations at Foils Engineering for hypergol based launch accident fireballs.

Reentry Analysis

Steep Trajectory Results: Globally converged RACER (flowfield) / LORAN-C (radiation) solutions have been obtained for the first five (out of ten) selected points on the steep (g = 90°) trajectory. Table 3-2 lists the freestream environment and imposed surface temperatures (based on SINRAP estimates) for the selected trajectory points. The temperatures for the fifth trajectory point are subject to change because the SINRAP solution has not been extended beyond the third point.

Table 3-2. Steep Trajectory Cases

Trajectory Point	Time (sec)	Velocity (kft/sec)	Altitude (kft)	T_{front} (°R)	T_{side} (°R)
1	0.0	63.834	258.000	2360	2330
				2410	2380
				2460	2430
2	0.3	63.762	238.864	3460	2460
				3960	2760
				4460	3060
3	0.6	63.586	219.764	5960	2560
				6460	2960
				6960	3360
4	1.1	62.752	188.149	6460	2960
				6960	3460
				7460	3960
5	1.6	60.214	157.306	6960	3460
				7460	3960
				7610	4110

In Figure 3-1, the prescribed front-face wall temperatures for the steep trajectory are compared to the converged SINRAP transient heating solution for the shallow (7°) trajectory. High wall temperatures (>7000°R) are reached in about one second on the steep trajectory. Along the shallow trajectory, it takes almost sixteen seconds to reach this elevated wall temperature.

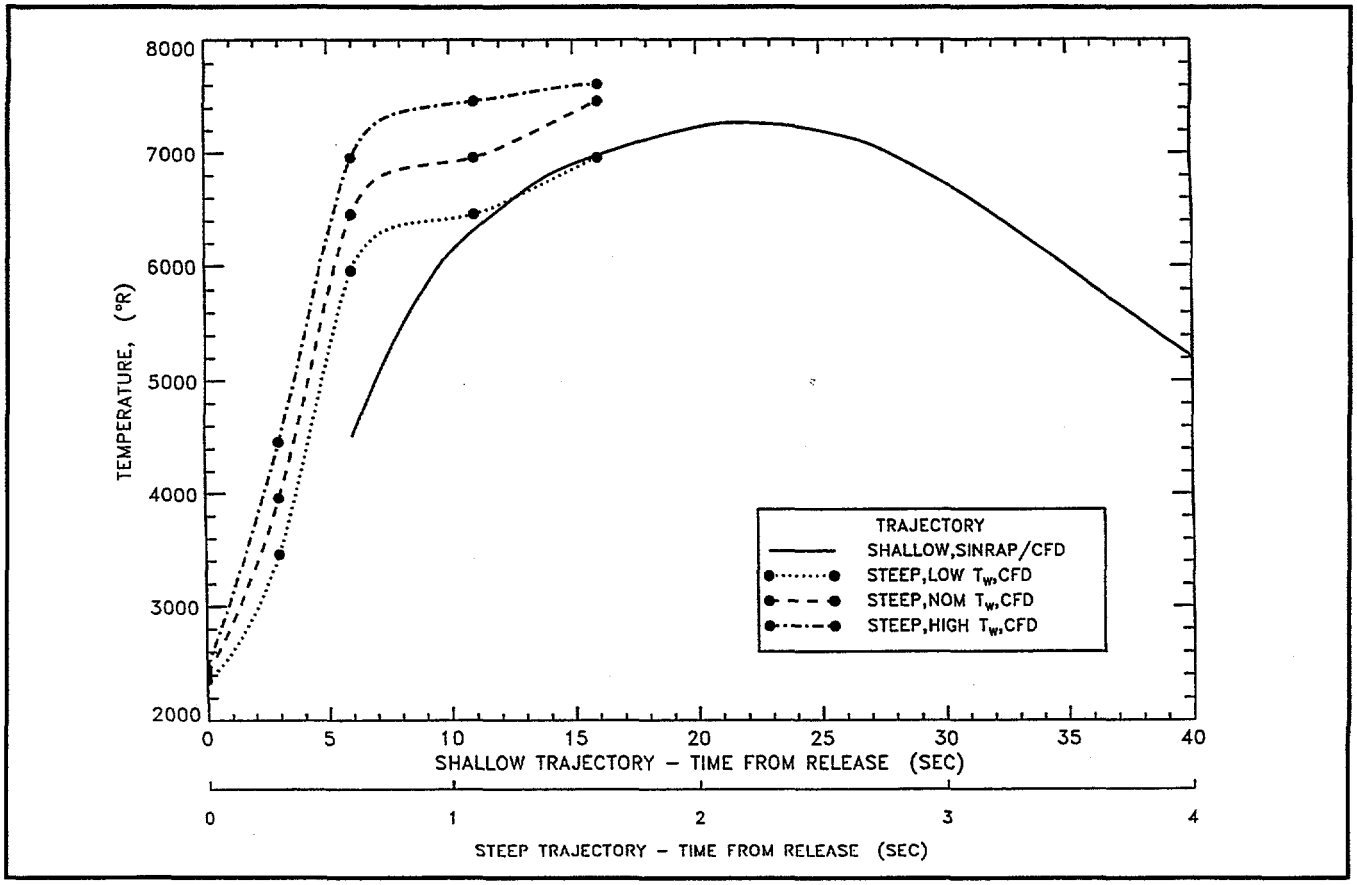

Figure 3-1. Steep Trajectory Computational Matrix. Comparison with Converged SINRAP Temperature History for the Shallow Trajectory

In Figures 3-2 through 3-4 the steep trajectory results are compared with the SINRAP shallow trajectory solution. The components of the heat flux are compared in Figure 3-2. The "convective" component includes gas conduction plus diffusion due to species gradients. As shown in Figure 3-2, the convective component is four to eight times higher (depending on wall temperature) for the steep, but the radiative component, at sixteen to eighteen times higher than the shallow, dominates. The total heat flux to the surface for the steep and shallow trajectories is shown in Figure 3-3. The total heat flux for the steep (at 1.6 seconds) is ten to thirteen times higher than shallow (at 16 seconds). The ablation rates are compared in Figure 3-4. The steep results, as expected, vary greatly with wall temperature. It is anticipated that the SINRAP converged wall temperature will lie close to the high wall temperature RACER/LORAN-C solution.

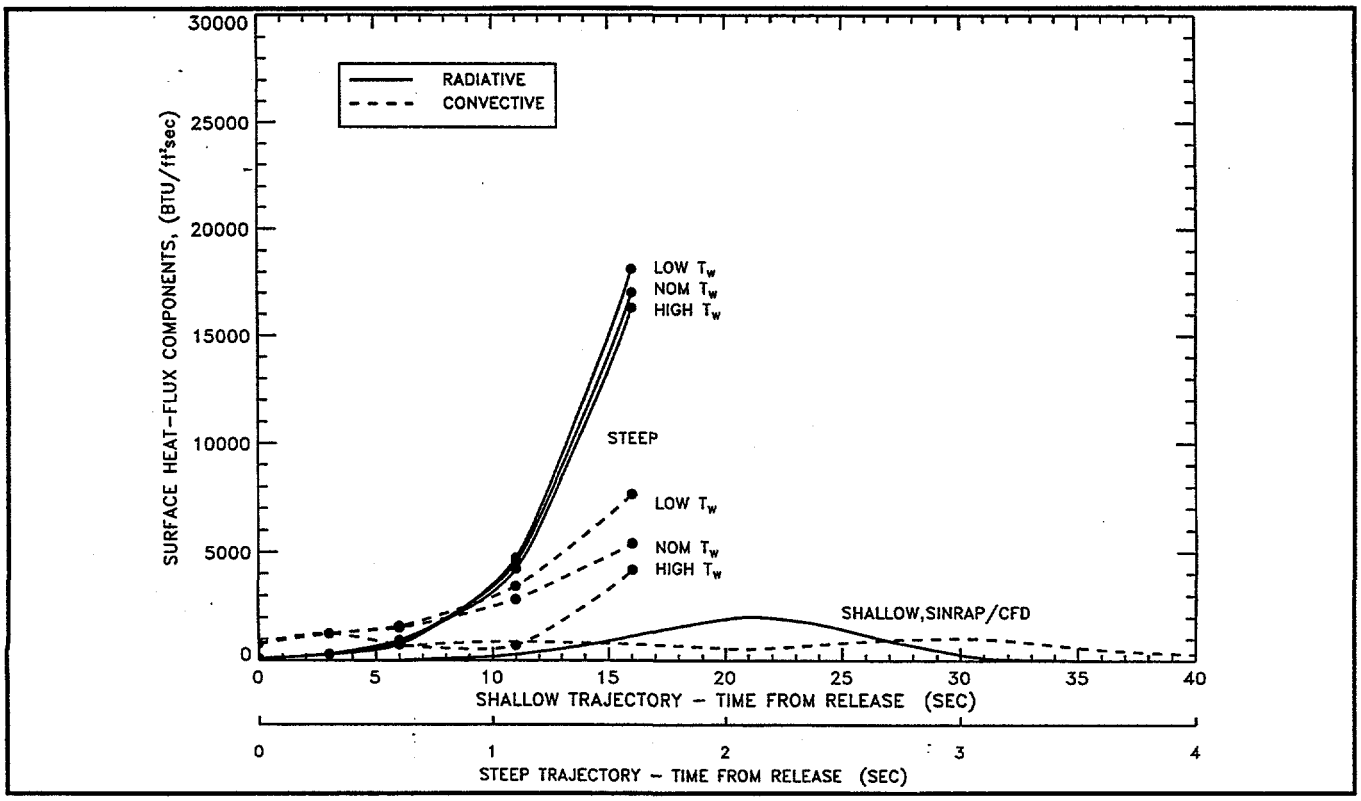

Figure 3-2. Comparison of the Heat Flux Components along the Steep Trajectory with the SINRAP Shallow Trajectory Solution

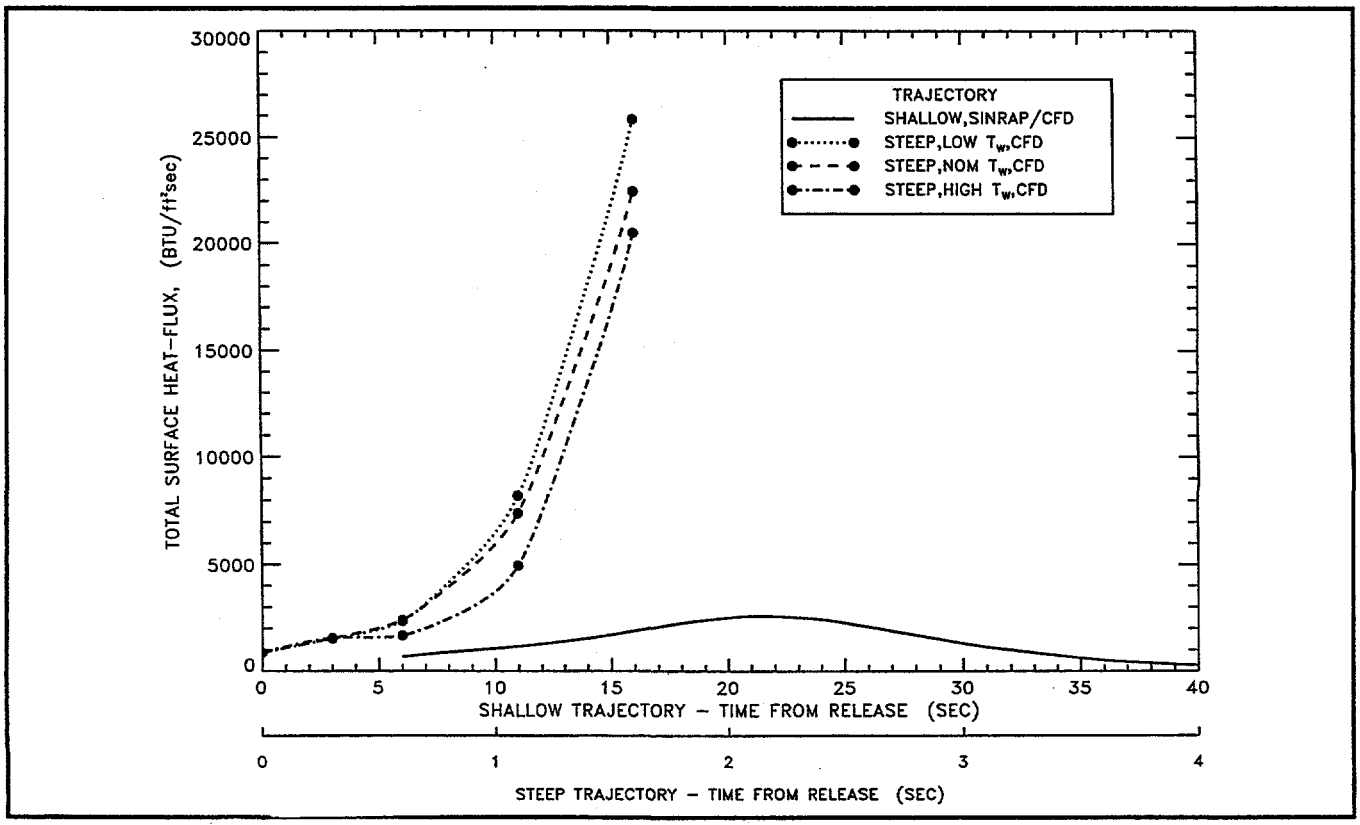

Figure 3-3. Comparison of the Total Heat Flux along the Steep Trajectory with the SINRAP Shallow Trajectory Solution

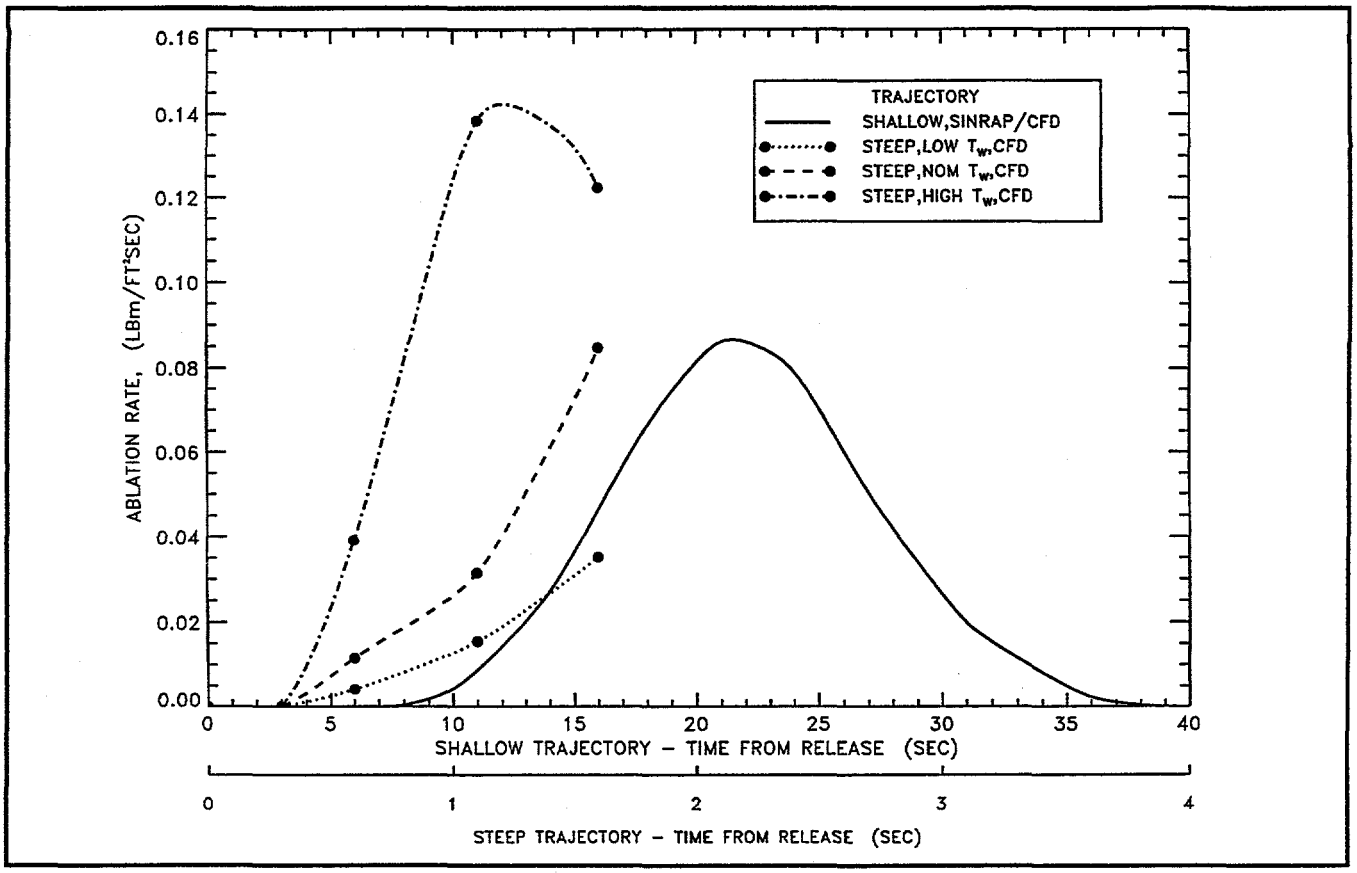

Figure 3-4. Comparison of the Ablation Rate along the Steep Trajectory with the SINRAP Shallow Trajectory Solution

Detailed flow and chemistry results along the stagnation streamline are compared in Figures 3-5 through 3-8. The shallow peak heating case (M_∞ = 50.7, altitude = 58.6 Km, T_w = 7260°R) is compared with the high wall temperature, case 5, on the steep trajectory (M_∞ = 55.9, altitude = 48.0 Km, T_w = 7610°R). The stagnation streamline pressure distributions are shown in Figure 3-5. The shock layer pressure is about four atmospheres for the steep but less than one atmosphere for the shallow. The shock layer temperature for the steep case, shown in Figure 3-6, reaches nearly 22,000°K (39,600°R). The peak shock layer temperature for the shallow case is less at about 18,000°K (32,400 °R). The stagnation streamline density, shown in Figure 3-7, is over four times higher for the steep case. The stagnation streamline carbon species distributions (with mass fractions greater than 0.001) are shown for the shallow and steep cases in Figures 3-8 and 3-9, respectively. Although the ablation rates are higher for the steep case, the carbon species penetrate farther into the shock layer for the shallow peak heating condition because of its lower density.

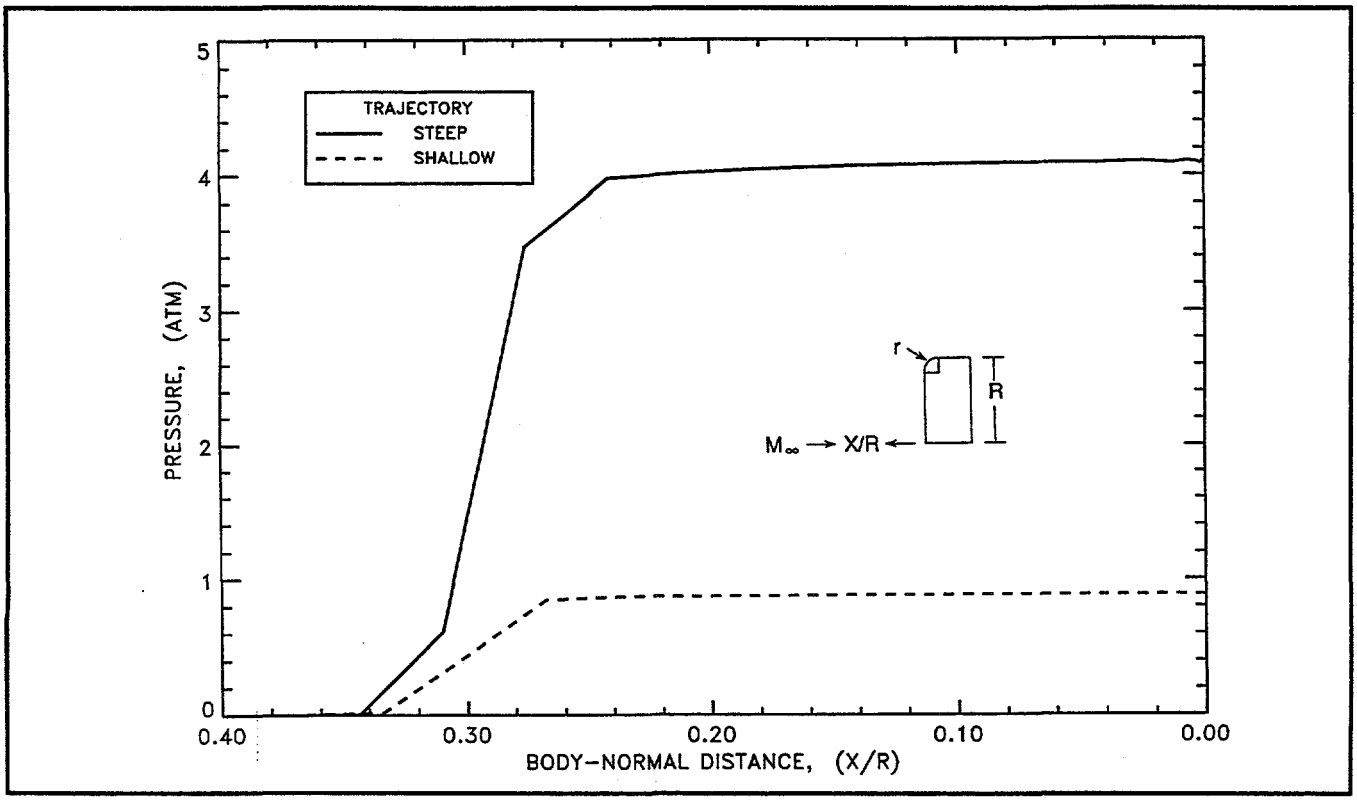

Figure 3-5. Stagnation Streamline Pressure Distribution. Comparison of Steep Case 5 (High T_w) with Shallow Peak Heating

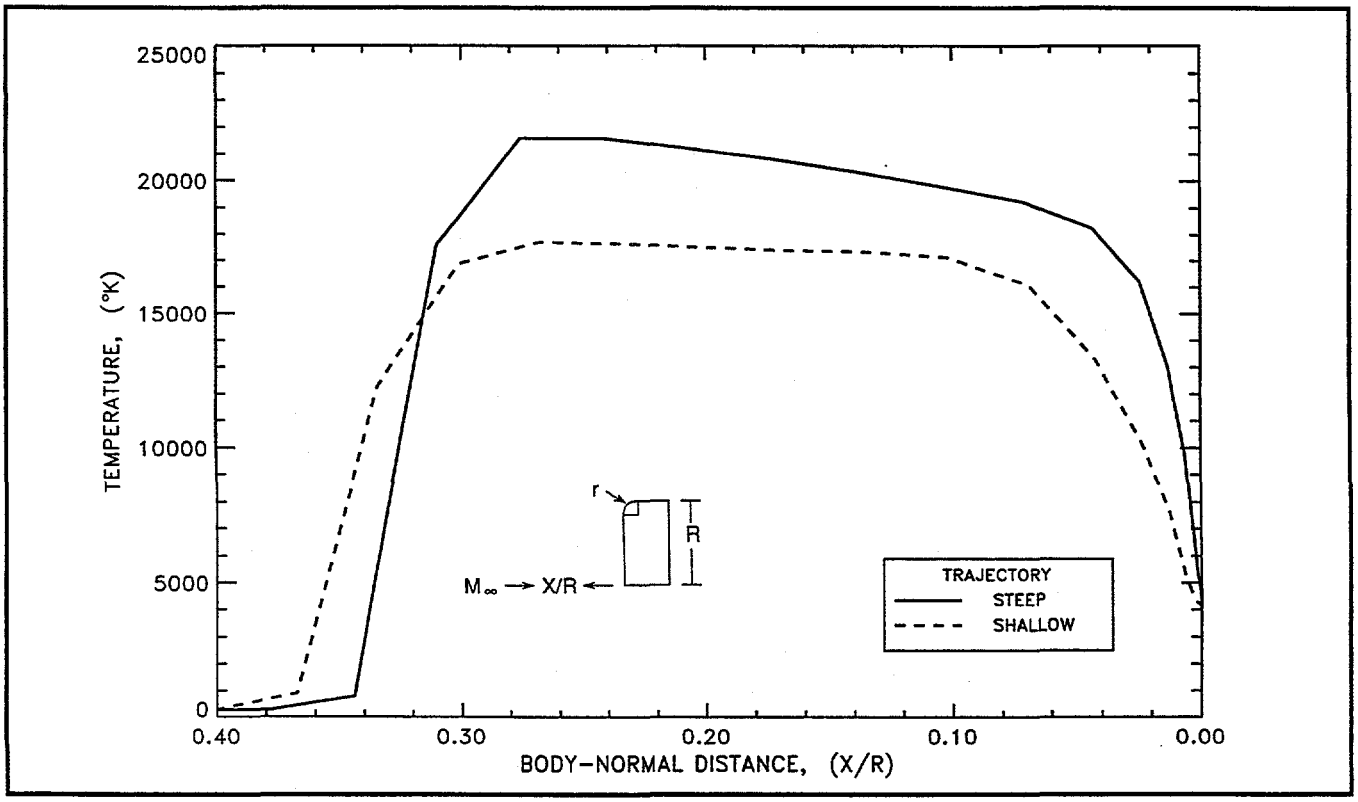

Figure 3-6. Stagnation Streamline Temperature Distribution. Comparison of Steep Case 5 (High T_w) with Shallow Peak Heating

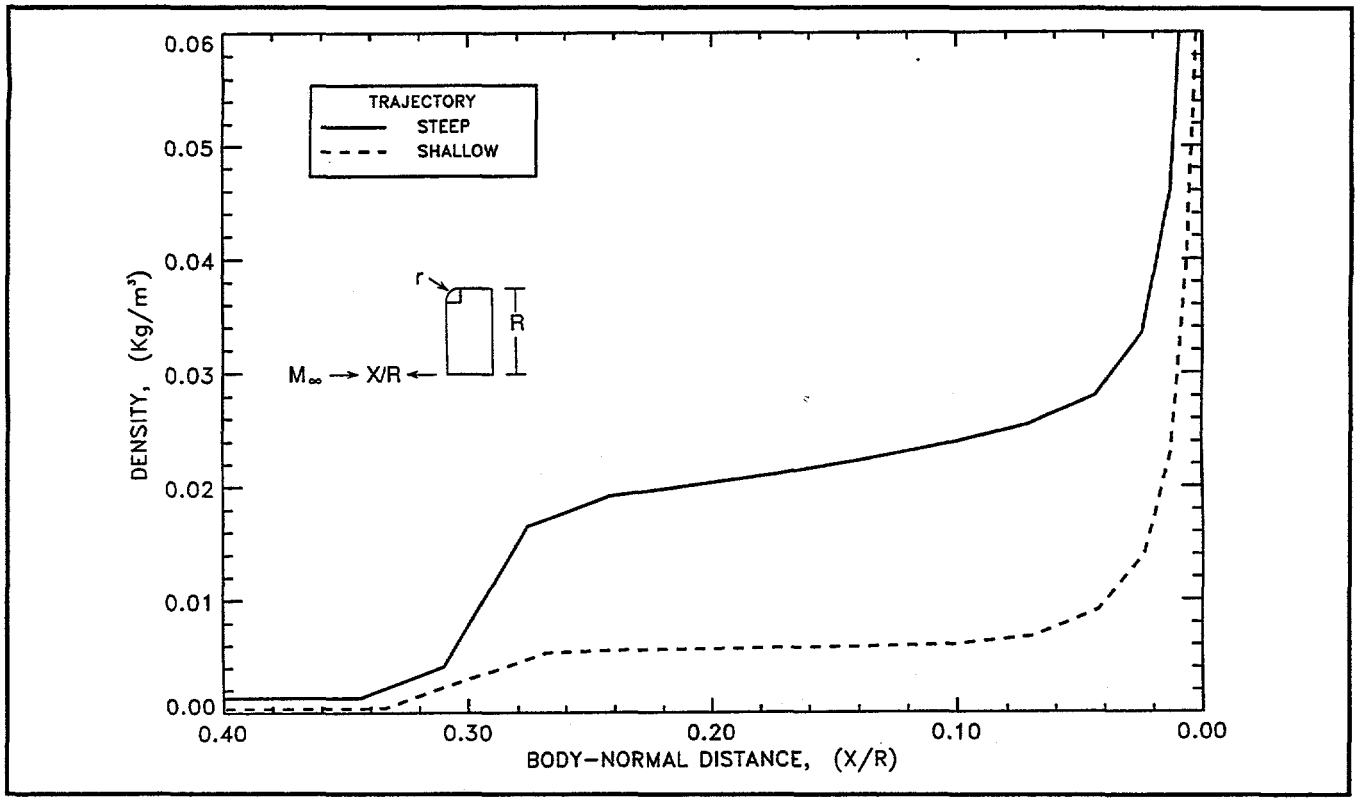

Figure 3-7. Stagnation Streamline Density Distribution. Comparison of Steep Case 5 (High T_w) with Shallow Peak Heating

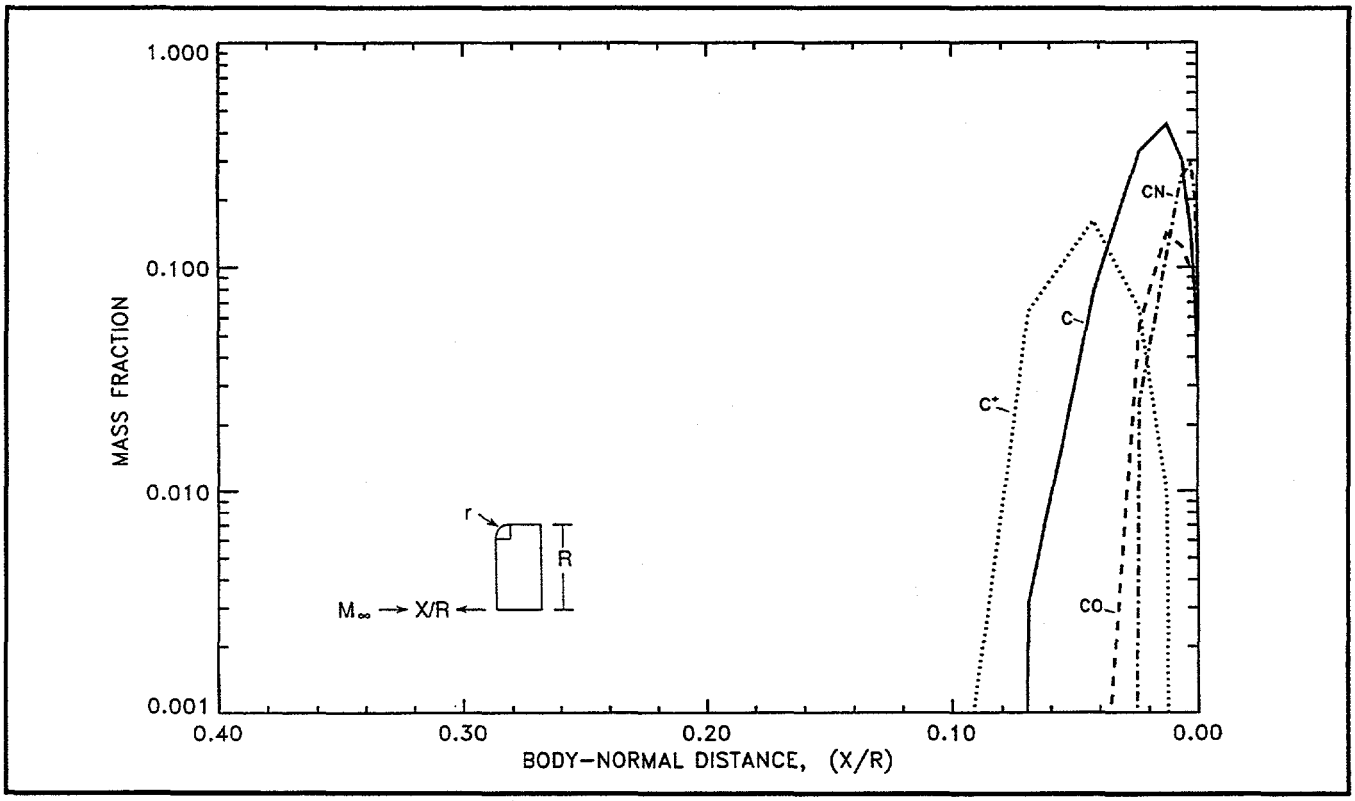

Figure 3-8. Carbon Species along the Stagnation Streamline. Shallow Peak Heating Solution

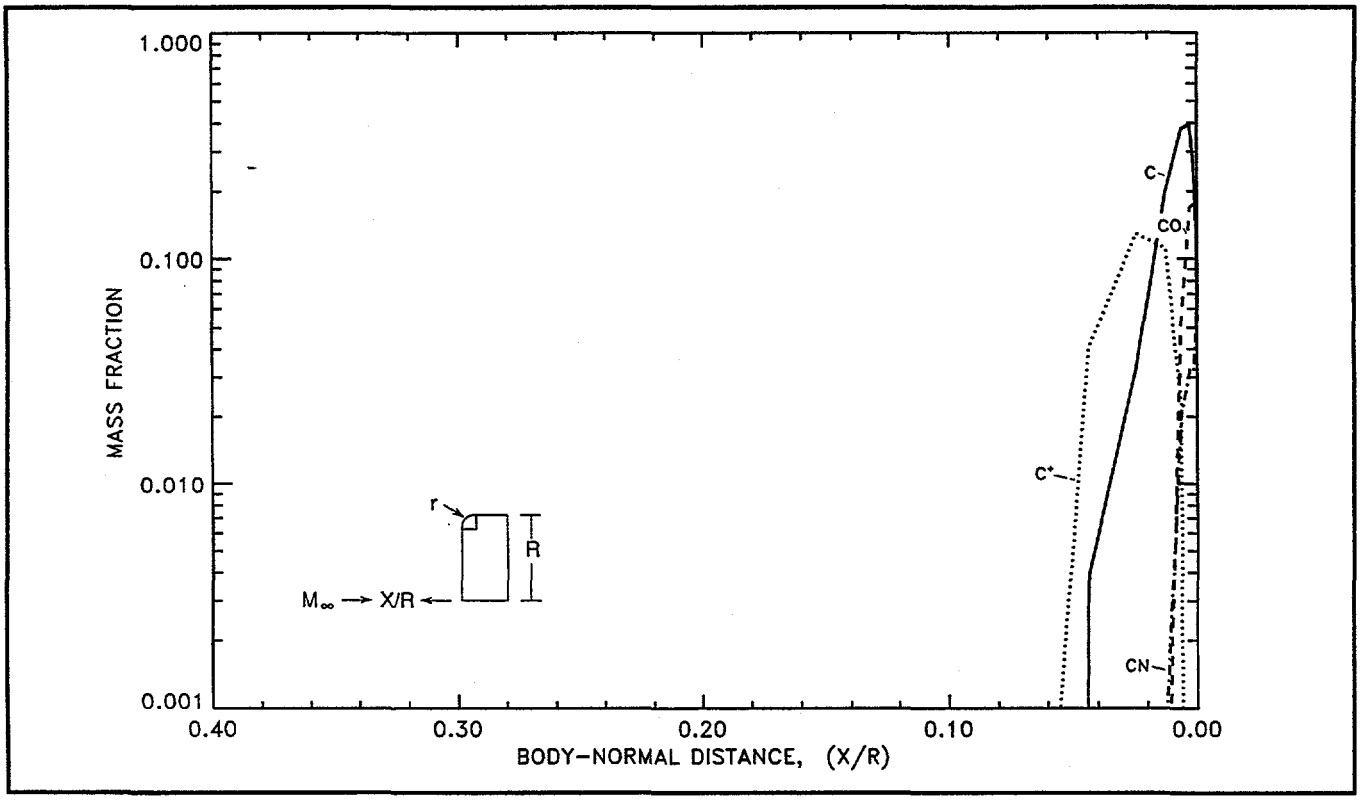

Figure 3-9. Carbon Species along the Stagnation Streamline. Steep Case 5 (High T_w) Solution

Heterogeneous Oxidation: Comments/questions from the Reentry Subpanel (Re: 27 October 1995 INSRP/RESP meeting) noted that, in the low temperature limit, the predicted ablation rate for the shallow trajectory cases was not consistent with the expected oxidation controlled, diffusion limit.

Because the RACER code applications were expected to lie within the sublimation regime, heterogeneous oxidation was not modeled. To insure that the "sublimation only" model did not adversely affect the SINRAP prediction of GPHS performance, the RACER code was modified to include heterogeneous oxidation. Case 4 on the shallow trajectory, with four wall temperature distributions, was repeated. As shown in Figure 3-10, the contribution of the heterogeneous oxidation reactions is only present at the lowest wall temperatures. For all cases of interest for SINRAP analyses of the shallow trajectory, heterogeneous oxidation is negligible (the integrated effect is less than 1 mil). However, the heterogeneous oxidation terms will be retained in the code and computed in all future analyses.

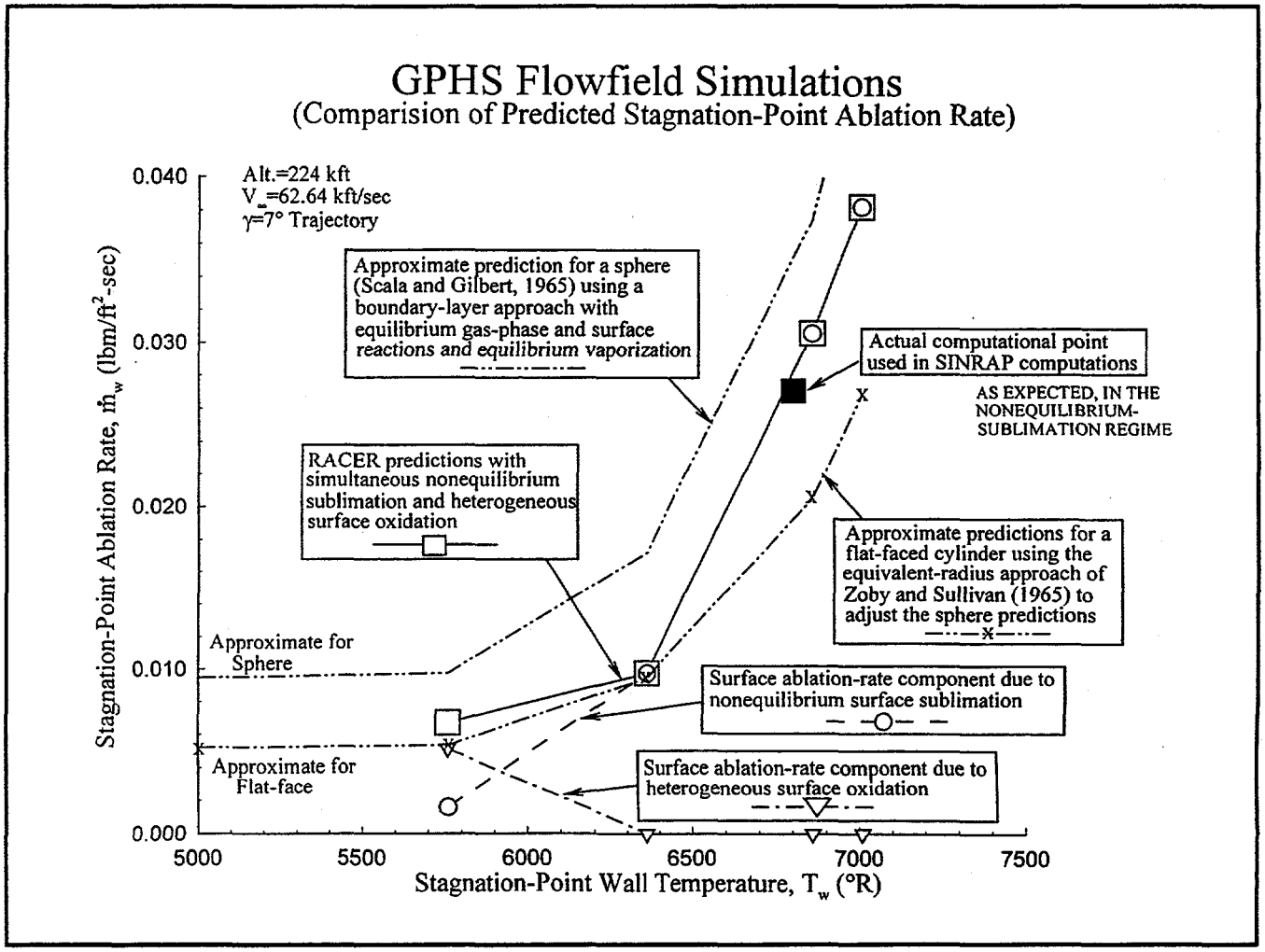

Figure 3-10. Effect of the Addition of Heterogeneous Surface Oxidation on the Ablation Rate. Shallow Trajectory, Point 4.

Work in Progress: The RACER/LORAN-C codes will continue to be applied along the steep trajectory. An approach has also been developed to address variability and uncertainty in the RACER and LORAN-C predictions. Implementation details will be developed over the next two months.

Reentry Thermal Analysis

The results for the shallow case are summarized herein. A presentation including these results is in the process of being prepared for the INSRP RESP meeting to be held 13-14 February 1996 at Aerospace Corporation in El Segundo, CA. Preliminary results for the steep case will also be presented.

Shallow Trajectory: The results which follow for the shallow case are:

- Summary of CFD Results
- Stagnation Node Temperature Results
- Recession Results
- Summary of Converged SINRAP Results
- Temperature and Recession Front Face Results at Peak Heating
- Temperature and Recession Results at 40 Seconds
- Stagnation Node Temperature and Recession Up to 100 Seconds
- Summary

Note: Results are based on SINRAP Rev. C which incorporates CFD output and material property changes

Table 3-3 summarizes the CFD results at the stagnation point. Figure 3-11 shows the stagnation node temperature as calculated by SINRAP and the imposed surface temperatures for the CFD runs as a function of altitude. Except for the first trajectory point, SINRAP converged to temperatures within the imposed range for the CFD cases.

Figure 3-12 shows the same stagnation node temperatures versus time. Figure 3-13 shows the average front face recession versus time and the results from the previous analysis (old). The new recession curve based on CFD output to 40 seconds shows that the recession is starting to level off. Table 3-4 shows coverged SINRAP results for the stagnation point at the times and altitudes of the eleven trajectory points chosen for CFD analysis. This summary was made to ensure that the converged values were reasonable in relation to CFD output as a function of temperature.

Table 3-3. Summary of CFD Results at Stagnation Point

Trajectory Point #	Time (Sec)	Altitude (Ft)	Surface Temperature (°F)	$Q_{RAD}\left(\frac{Btu}{Ft^2 \cdot S}\right)$	$Q_{CONV}\left(\frac{Btu}{Ft^2 \cdot S}\right)$	$\dot{m}\left(\frac{lbm}{Ft^2 \cdot S}\right)$	$\sum_{i=1}^{3} m_{i\omega} h_{i\omega}\left(\frac{Btu}{Ft^2 \cdot S}\right)$
1	6	273219	4700	57	548	.00006	1
			5300	112	453	.0016	29
			5900	140	232	.0099	168
2	8	259936	4700	74	815	.00006	1
			5300	111	735	.0016	29
			5900	172	475	.0087	148
3	10	247344	4700	184	1049	.00006	1
			5300	190	942	.0016	29
			5900	171	791	.0089	151
			6400	245	57	.0514	873
4	14	224381	5300	616	1534	.0016	29
			5900	716	1416	.0097	166
			6400	715	754	.0310	521
			6550 *	636	124	.0383	654
5	18	204690	5300	1533	2054	.0016	29
			5900	1628	1965	.0116	197
			6400	1571	1435	.0278	474
			6800	1567	235	.1102	1882
6	21	192254	5900	2081	2134	.0126	214
			6400	2126	1717	.0279	476
			6800	2052	556	.0843	1441
7	24	181830	6400	1685	1591	.0280	477
			6680	1716	1005	.0567	969
			6900	1676	373	.1207	2061
8	27	173266	6265	965	1477	.0227	385
			6600	918	1003	.0474	810
			6865	1027	358	.1036	1770
9	31	164264	5800	106	1267	.0130	228
			6250	118	956	.0228	388
			6600	142	582	.0491	838
10	36	155858	5040	0	510	.0004	8
			5600	0	498	.0065	120
			6040	0	461	.0150	254
11	40	150641	4800	0	272	.00010	2
			4968	0	269	.00027	5
			5100	0	266	.00056	11

* Not used in SINRAP analyses

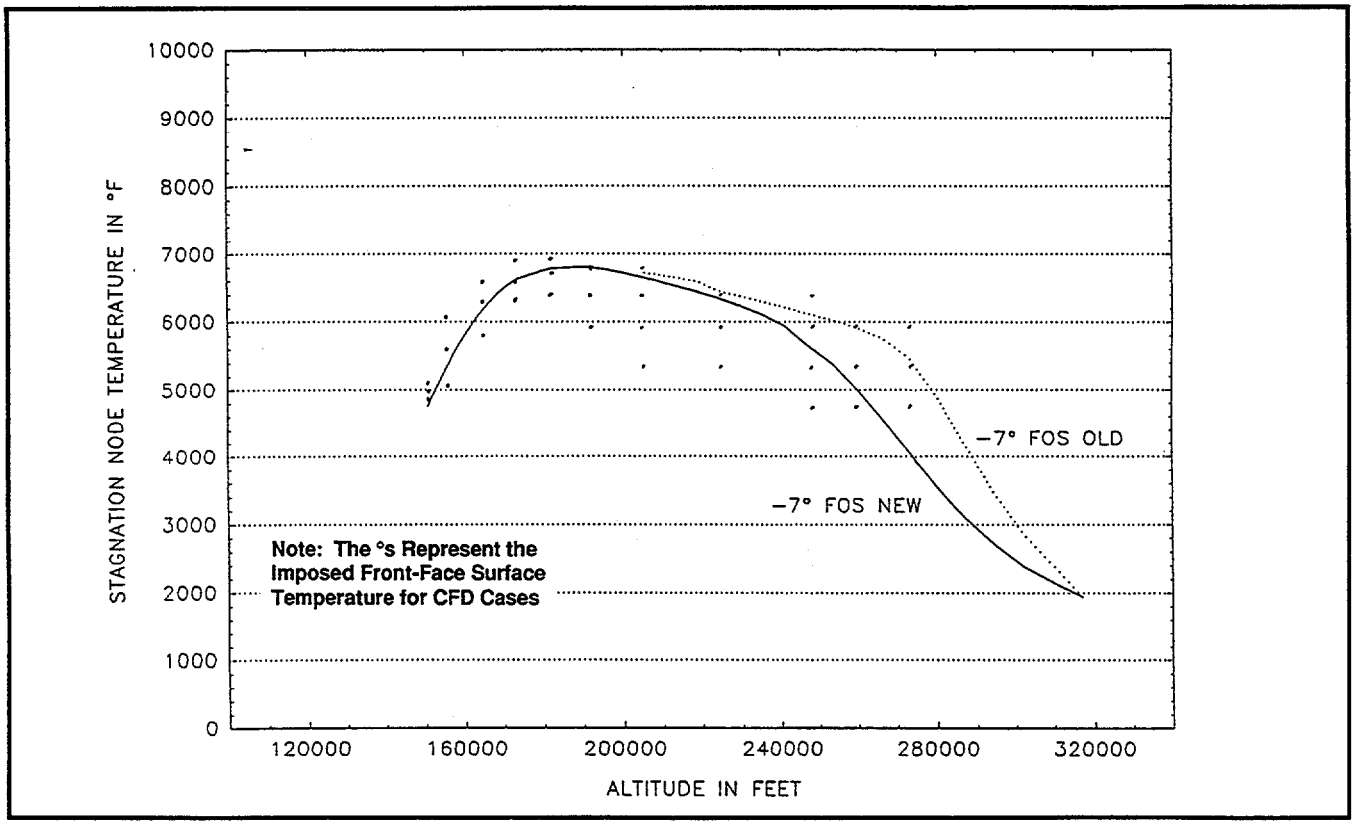

Figure 3-11. Stagnation Node Temperature Vs. Altitude

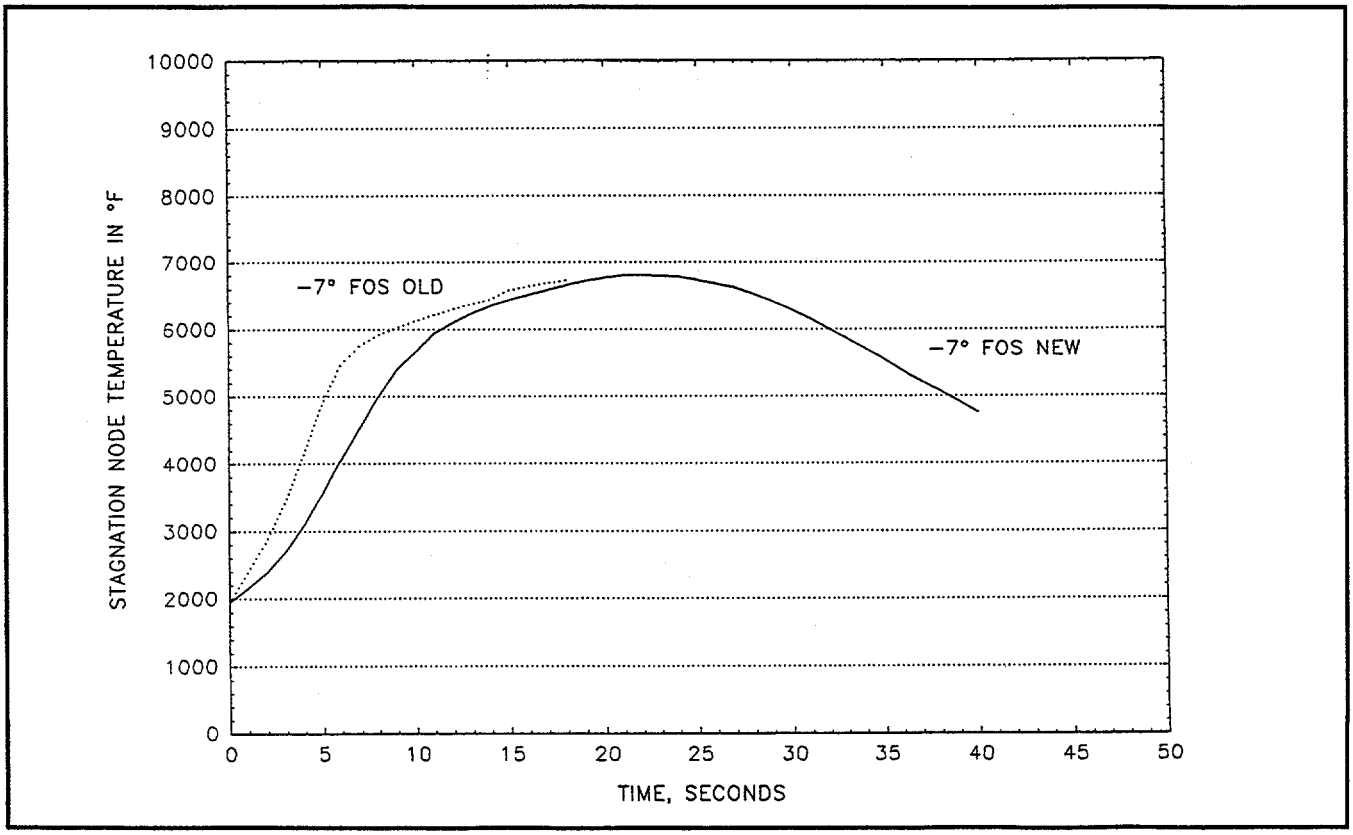

Figure 3-12. Stagnation Node Temperature Vs. Time

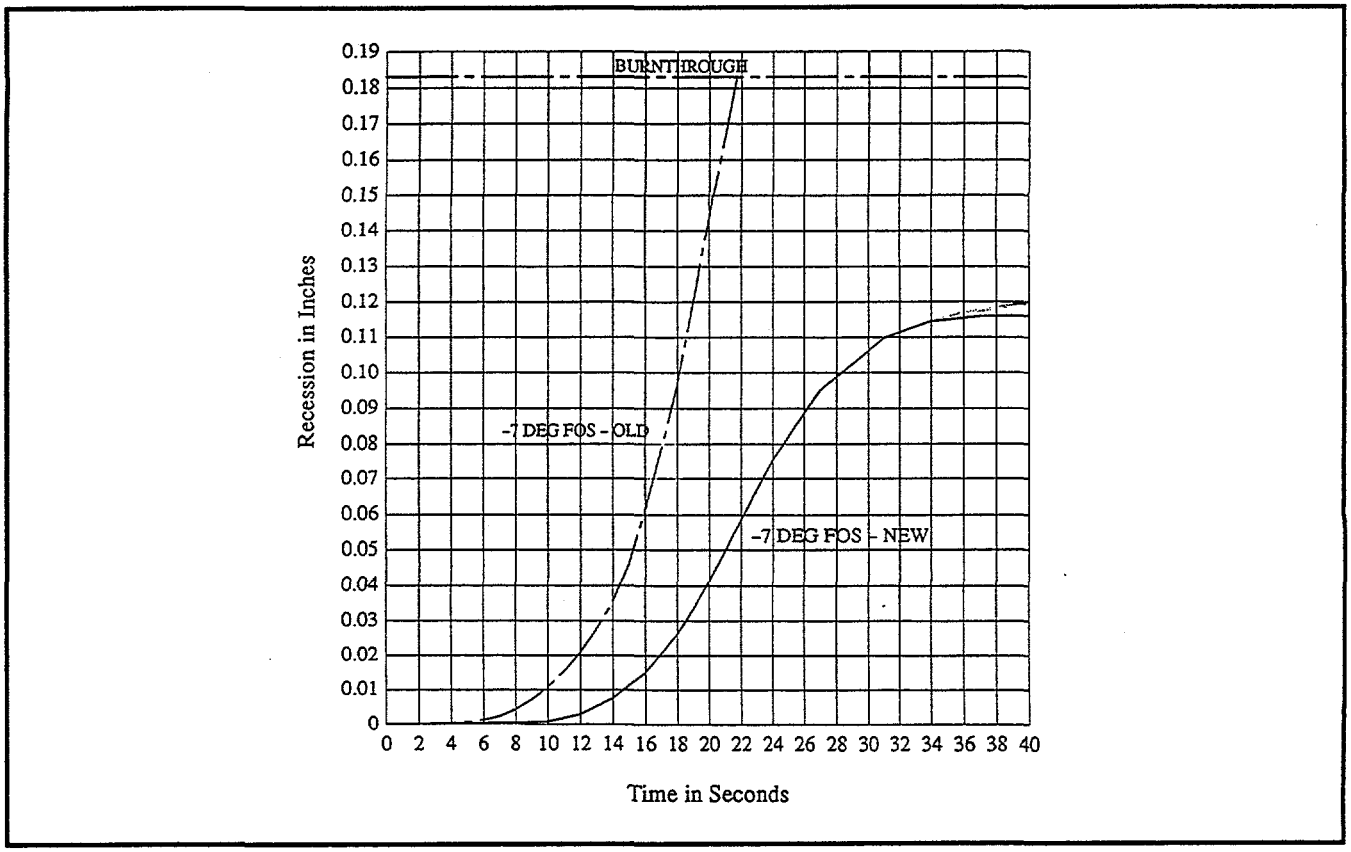

Figure 3-13. Front Face Average Recession - Face-On Stable

Table 3-4. Summary of Converged SINRAP Results for Stagnation Point

Trajectory Point #	Time (Sec)	Altitude (Ft)	Surface Temperature (°F)	$Q_{RAD}\left(\frac{Btu}{Ft^2 \cdot S}\right)$	$Q_{CONV}\left(\frac{Btu}{Ft^2 \cdot S}\right)$	$\dot{m}\left(\frac{lbm}{Ft^2 \cdot S}\right)$	$\sum_{i=1}^{3} m_{i\omega} h_{i\omega}\left(\frac{Btu}{Ft^2 \cdot S}\right)$
1	6	273219	4050	0	665	.0000016	.03
2	8	259936	5001	92	791	.00031	6.0
3	10	247344	5651	175	880	.00429	75
4	14	224381	6344	711	826	.0271	462
5	18	204690	6658	1573	681	.0663	1311
6	21	192254	6804	2041	542	.0862	1473
7	24	181830	6778	1692	733	.0792	1354
8	27	173266	6622	927	962	.0504	861
9	31	164264	6149	114	1017	.0199	341
10	36	155858	5373	0	508	.00226	42
11	40	150641	4751	0	275	.000078	2

Figure 3-14 shows the twenty front face nodes with only six nodes near the stagnation point having the minimum thickness of 0.185". Figures 3-15 and 3-16 show the temperature and corresponding recession of the front face nodes at 21 seconds, the time of peak heating. The variation in temperature and recession over the front-face is small. Figures 3-17 and 3-18 show temperatures and corresponding recession at 40 seconds. Again, the variation is small. Figure 3-19 shows temperature and recession up to 100 seconds. At 40 seconds, CFD output ended, and SINRAP used classical methods to determine convection and ablation. There is an obvious change in the curves when this occurs. The ablation curve suggests that an earlier shift from CFD to SINRAP would have precluded the small discontinuity seen at 40 seconds. The calculated take off temperature to the sublimation regime was calculated to be approximately 5000°F at 38 seconds. To determine the effect of the ablation curve discontinuity, an alternate run was made with CFD ending at 38 seconds. For this run, after 48 seconds the temperature calculated was within 2°F of the baseline run and the recession was only 2 mils greater. This indicates that the small discontinuity has a negligible effect on cumulative ablation. The shallow trajectory SINRAP run is being completed to impact for determination of aeroshell temperature upon ground impact.

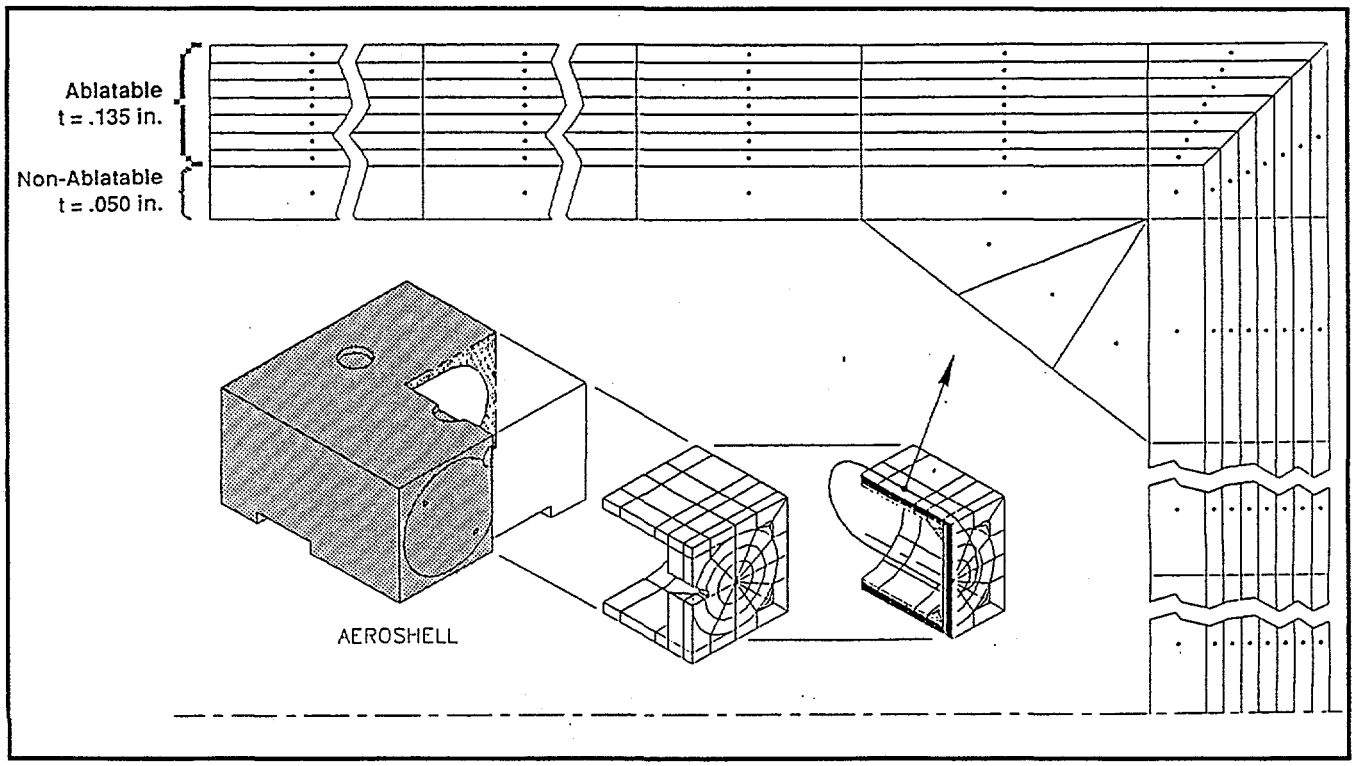

Figure 3-14. SINRAP Nodal Definition through Aeroshell

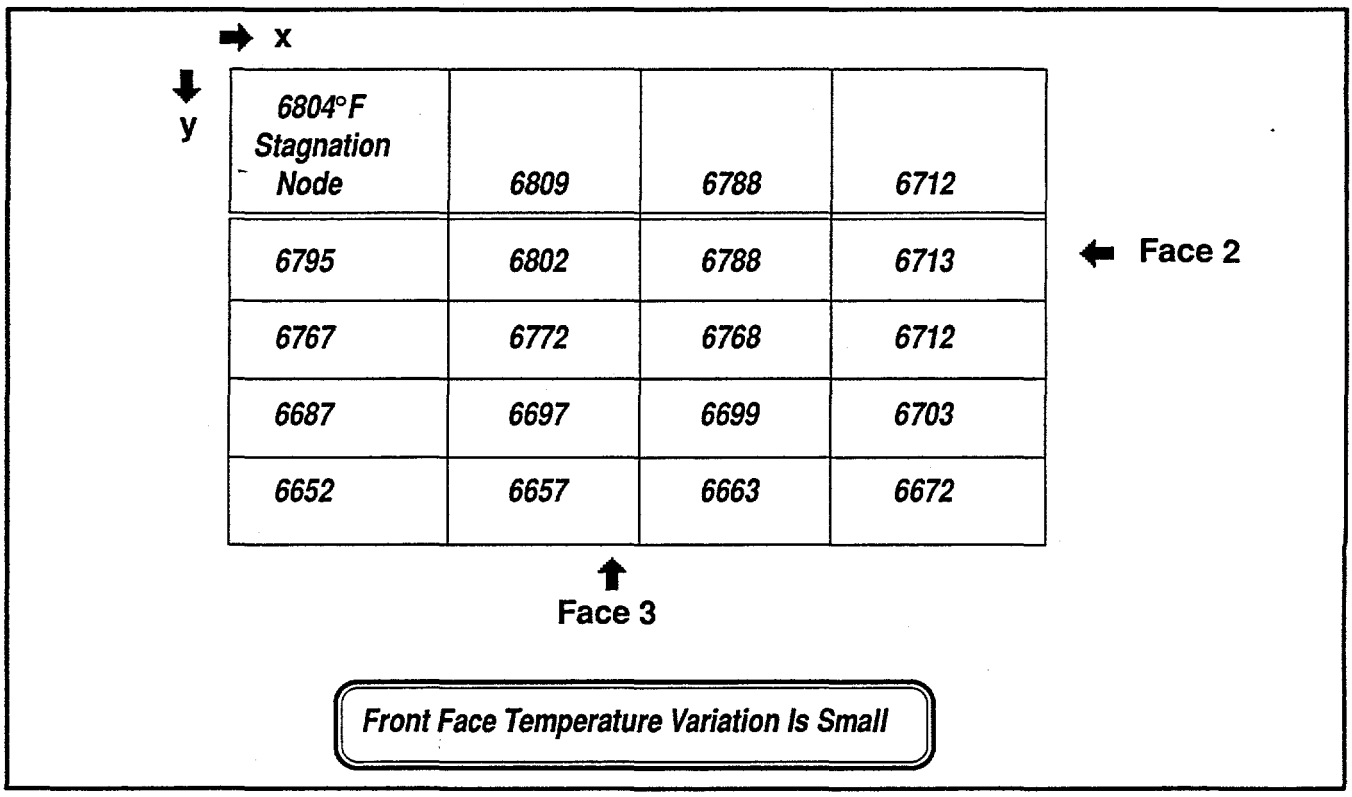

Figure 3-15. Aeroshell Front Face Temperatures at 21 Seconds

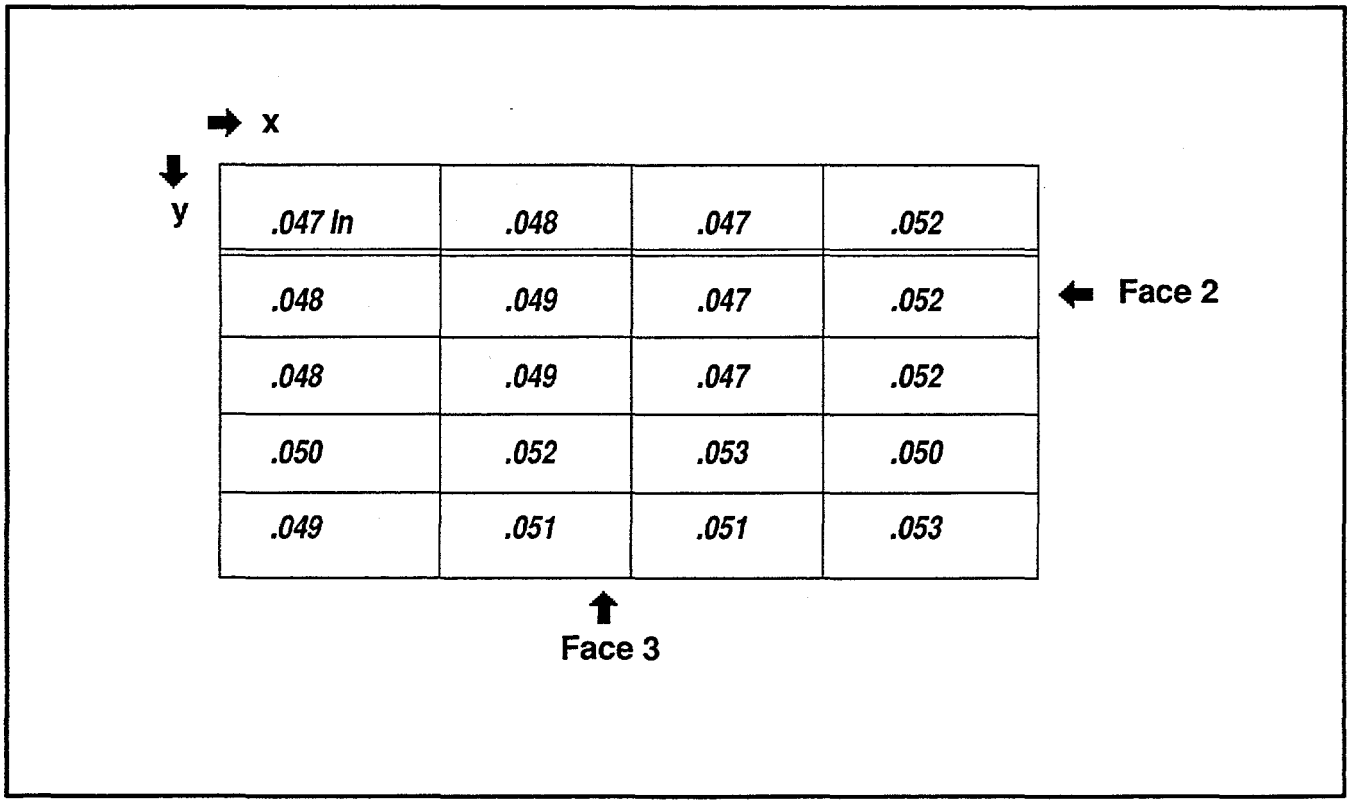

Figure 3-16. Aeroshell Front Face Recession at 21 Seconds

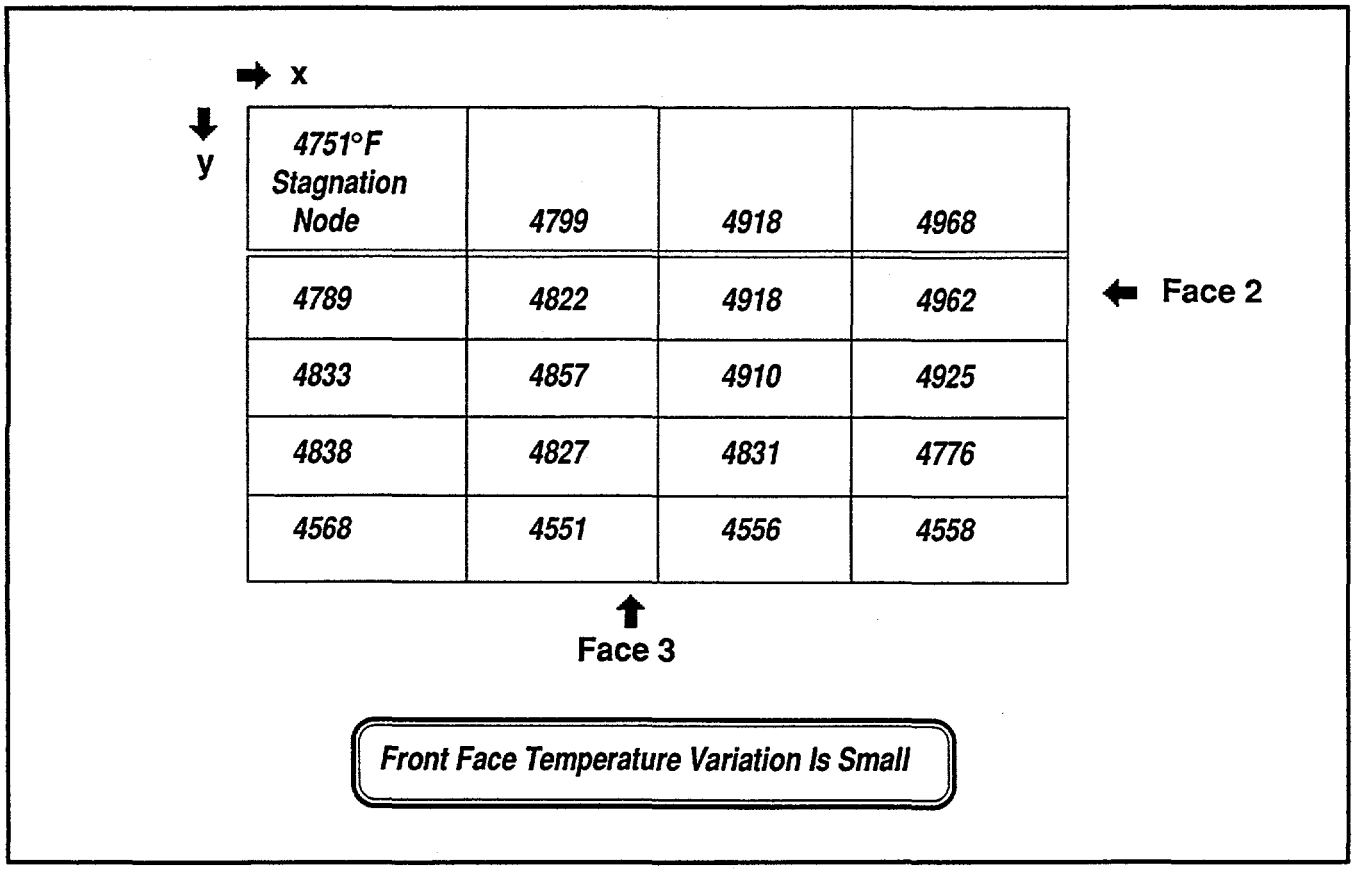

Figure 3-17. Aeroshell Front Face Temperatures at 40 Seconds

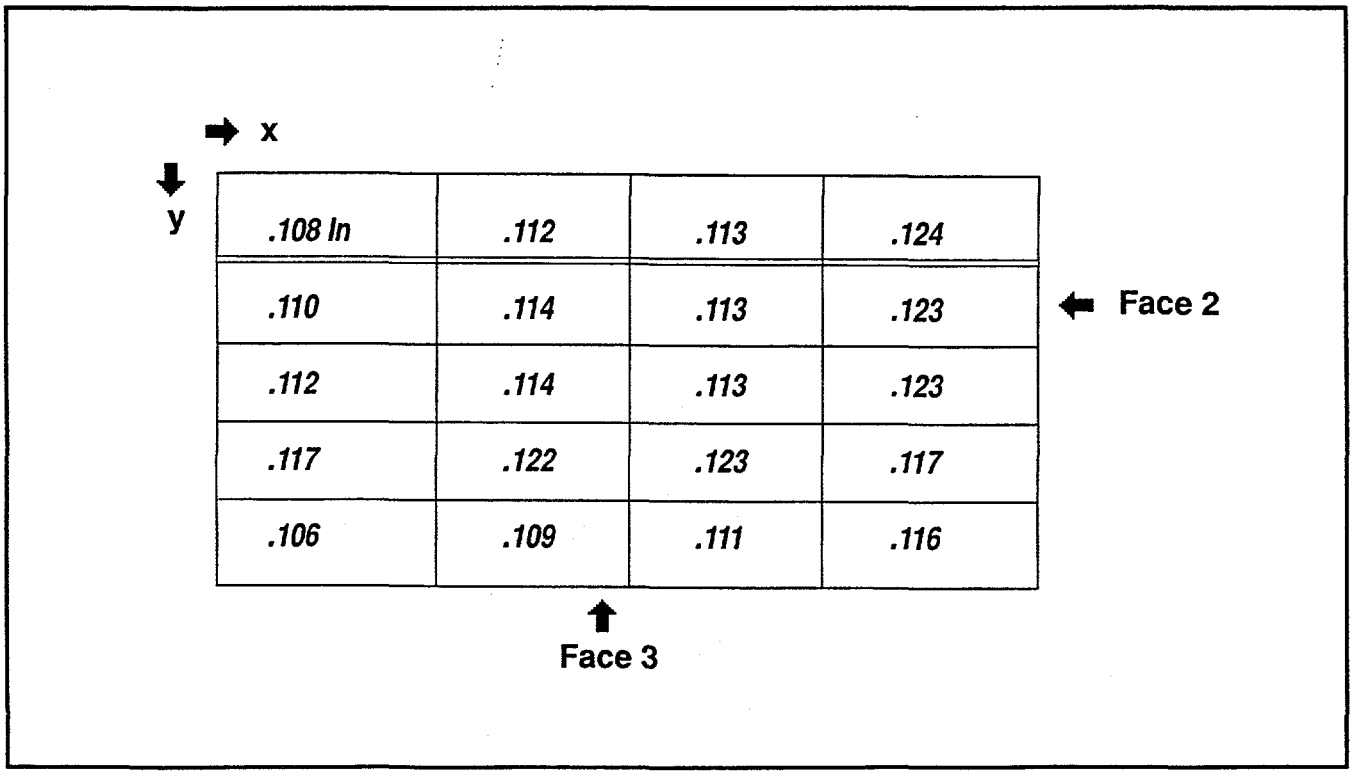

Figure 3-18. Aeroshell Front Face Recession at 40 Seconds

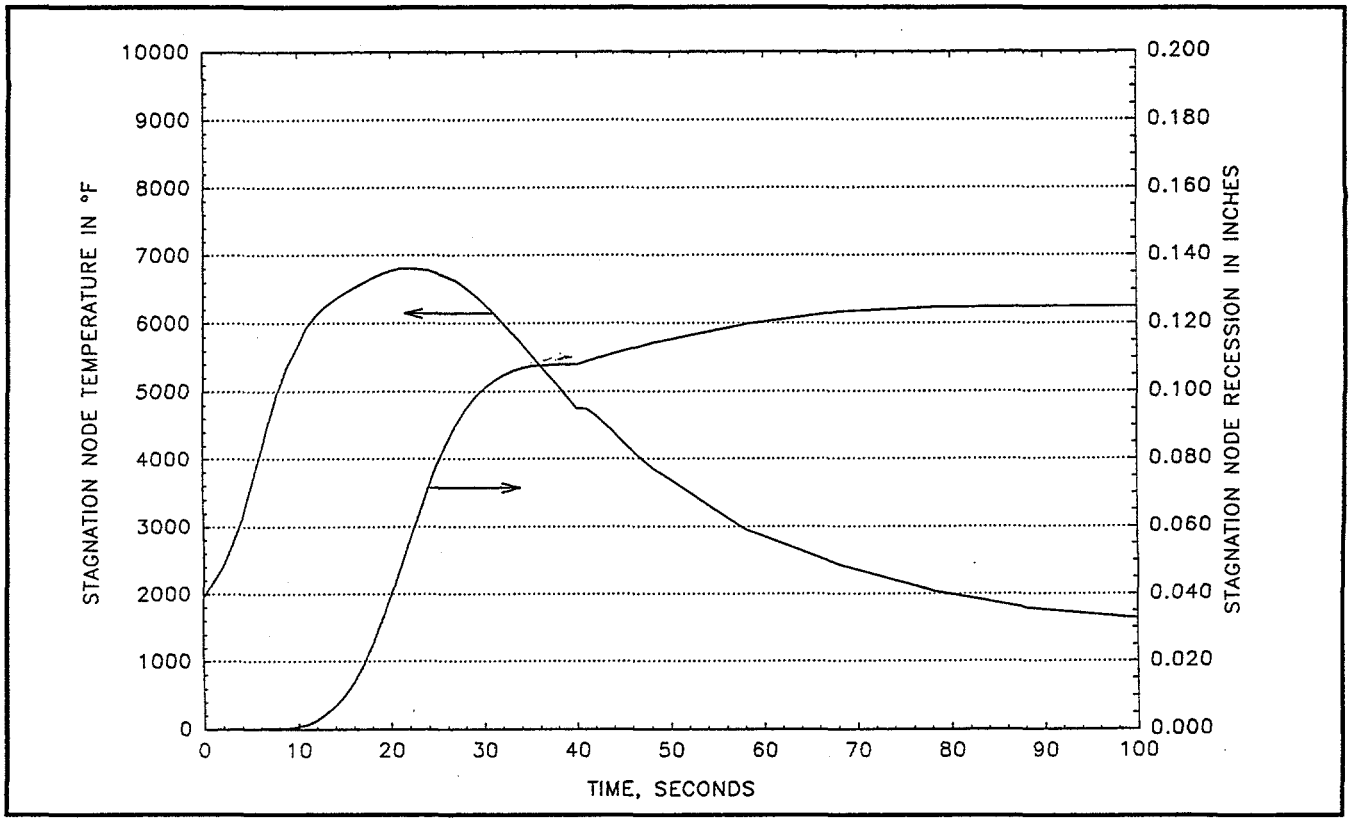

Figure 3-19. Stagnation Node Temperature and Recession Vs. Time

Shallow Trajectory: (Cont'd)

In summary, for the shallow trajectory,

- CFD analysis results have been successfully incorporated into SINRAP.
- The resulting aeroshell ablation is significantly lower than predicted by previous analyses.
- At surface temperatures below those of the sublimation regime, or post CFD ablation continues at a decreasing rate until a surface temperature of about 2000°F is reached.
- Burn-through of the aeroshell does not occur for the face-on stable orientation for the shallow trajectory under nominal conditions.

Steep Trajectory: For the steep trajectory, the CFD results for the first three trajectory points were incorporated into SINRAP. The calculated temperatures from SINRAP, along with results from the previous steep analysis, were used to impose CFD surface temperatures for the trajectory points 4 and 5. CFD output for the first five trajectory points is summarized in Table 3-5. For trajectory point 5, the original imposed high temperature was 7500°F, but to date, the highest CFD converged value is 7150°F.

Table 3-5. CFD Results at Stagnation Point - Steep Trajectory

Trajectory Point #	Time (Sec)	Altitude (Ft)	Surface Temperature (°F)	$Q_{RAD}\left(\frac{Btu}{Ft^2 \cdot S}\right)$	$Q_{CONV}\left(\frac{Btu}{Ft^2 \cdot S}\right)$	$\dot{m}\left(\frac{lbm}{Ft^2 \cdot S}\right)$	$\sum_{i=1}^{3} m_{i\omega} h_{i\omega}\left(\frac{Btu}{Ft^2 \cdot S}\right)$
1	0	258000	1900	94	774	.0	0
			1950	94	774	.0	0
			2000	93	774	.0	0
2	0.3	238864	3000	275	1245	.0	0
			3500	301	1252	.0	0
			4000	302	1257	.0	0
3	0.6	219764	4500	838	1739	.000016	0
			5500	806	1611	.0041	76
			6500	941	738	.0391	667
4	1.1	188149	6000	4752	3438	.0155	264
			6500	4554	2843	.0314	537
			7000	4225	715	.1384	2370
5	1.6	157306	6500	19617	8027	.0362	617
			7000	17412	5444	.0864	1490
			7150	17411	4559	.1217	2099

Based on the large increase in radiation from points 4 to 5, and extrapolation of SINRAP results incorporating points 1 through 3, it is likely that a surface temperature considerably higher than 7500°F will be required.

Reentry Structural Analysis

Analysis and documentation of the thermostructural analysis for the 7 degree (shallow) trajectory were completed. A summary of critical stresses and strains for the five baseline analysis points in this trajectory are provided in Table 3-6. Contours of stress and strain factors of safety for the t = 22 second and t = 26 second timepoints are shown in Figures 3-20 and 3-21, respectively. As was documented in the last monthly report, the baseline analysis results indicate sufficient capability in the GPHS aeroshell to survive reentry loads for this trajectory.

The effects of roll rate on aeroshell survivability were assessed by adding a centrifugal force to the model load conditions, as well as a distributed loading on the chamfer representing forces from the GIS. Flight dynamic analysis indicate that an envelope of potential roll rates exists for the aeroshell as a function of altitude based on various reentry trajectories. At the critical thermostructural analysis altitudes of 160 to 260 kft, these roll rates can range from 0 to 12000 deg/sec., with the higher rates occurring at the lower altitudes. At altitudes below 150 kft, roll rate predictions level out at approximately 15000 deg/sec. As a preliminary assessment on the effects of the roll, the maximum 15000 deg/sec roll rate was conservatively assumed to coincide with the worst case reentry condition at t = 22 seconds. A comparison of critical stresses for the roll versus no-roll cases at t = 22 seconds indicated that roll rate had little impact on the peak stresses in the aeroshell, with a reduction in the minimum factor of safety from 1.467 to 1.460. Analysis at the t = 8 seconds flight conditions with the 15000 deg/sec roll rate demonstrated a similarly negligible impact. The aeroshell stresses due to roll were assessed independently of any other loads and found to be relatively benign. The effects of the roll loads are concentrated in the chamfer and the aeroshell sidewall areas, which are relatively thick, and not in the forward face of the aeroshell where the critical thermostructural stresses occur.

Documentation of all thermostructural analyses for the shallow trajectory was completed. The analysis report includes extensive discussion of the ABAQUS finite element model and the nonlinear constitutive material model, as well as the analytical methodology and the load conditions for the 7 degree trajectory. Results are included for the baseline analysis, the assessment of roll loads, and the calculation of relative deflections between the GIS and the aeroshell.

Table 3-6. Summary of Stresses and Strains for the Cassini GPHS Aeroshell 7 Degree Face-On Stable Trajectory, No Roll

	Analysis Time (secs)				
	8	22	26	29	33
Flight Condition	Maximum Gradient	Maximum Temperature	Maximum Load	Intermediate Point	Critical Ablation
X DIRECTION					
Stress (ksi)	−11.11	−2.02	−2.12	−2.39	−3.38
Temperature (°F)	4825	6767	6652	6433	5942
Allowable (ksi)	−25.61	−2.97	−3.20	−3.84	−6.73
Factor of Safety	**2.305**	**1.467**	**1.504**	**1.608**	**1.992**
Strain (%)	0.09	−0.55	−0.62	−0.50	−0.27
Temperature (°F)	3161	6767	6652	6433	5942
Allowable (%)	0.42	−2.57	−2.40	−2.07	−1.44
Factor of Safety	**4.641**	**4.667**	**3.873**	**4.122**	**5.330**
Y DIRECTION					
Stress (ksi)	−12.19	−0.93	−1.69	−1.93	−3.26
Temperature (°F)	4297	6659	6366	6200	5525
Allowable (ksi)	−29.25	−3.18	−4.17	−5.00	−11.90
Factor of Safety	**2.400**	**3.434**	**2.468**	**2.589**	**3.652**
Strain (%)	0.09	−0.21	−0.25	−0.23	−0.14
Temperature (°F)	2804	6507	6366	6200	5903
Allowable (%)	0.37	−2.17	−1.98	−1.74	−1.42
Factor of Safety	**4.308**	**10.534**	**7.862**	**7.647**	**10.170**
Z DIRECTION					
Stress (ksi)	−13.40	9.35	7.16	−6.91	−7.57
Temperature (°F)	2648	4146	4523	4501	4197
Allowable (ksi)	−19.31	27.58	28.15	−28.49	−26.29
Factor of Safety	**1.441**	**2.951**	**3.930**	**4.125**	**3.471**
Strain (%)	−0.16	−0.16	−0.14	−0.12	−0.09
Temperature (°F)	2648	5760	5856	5749	4197
Allowable (%)	−0.32	−1.39	−1.41	−1.38	−1.02
Factor of Safety	**1.969**	**8.889**	**9.868**	**11.151**	**11.900**
SHEAR					
Stress					
Peak τ_{XY} (ksi)	2235	1408	1217	1122	1224
Peak τ_{XZ} (ksi)	2895	1053	980	1089	1156
Strain					
Peak γ_{XY} (%)	0.45	0.46	0.39	0.36	0.33
Peak γ_{XZ} (%)	0.69	0.73	0.90	0.84	0.54

Note: Factor of Safety = (Allowable Value)/(Predicted value)

Work in Progress: A thermostructural analysis document for the 7 degree trajectory will be issued following the review cycle and the incorporation of any required changes. In conjunction with this, the thermostructural analysis for the steep trajectory will be initiated when the SINRAP thermal analysis has progressed sufficiently to provide the necessary inputs. An approach for the treatment of variability and uncertainty in the structural analysis work is also under development.

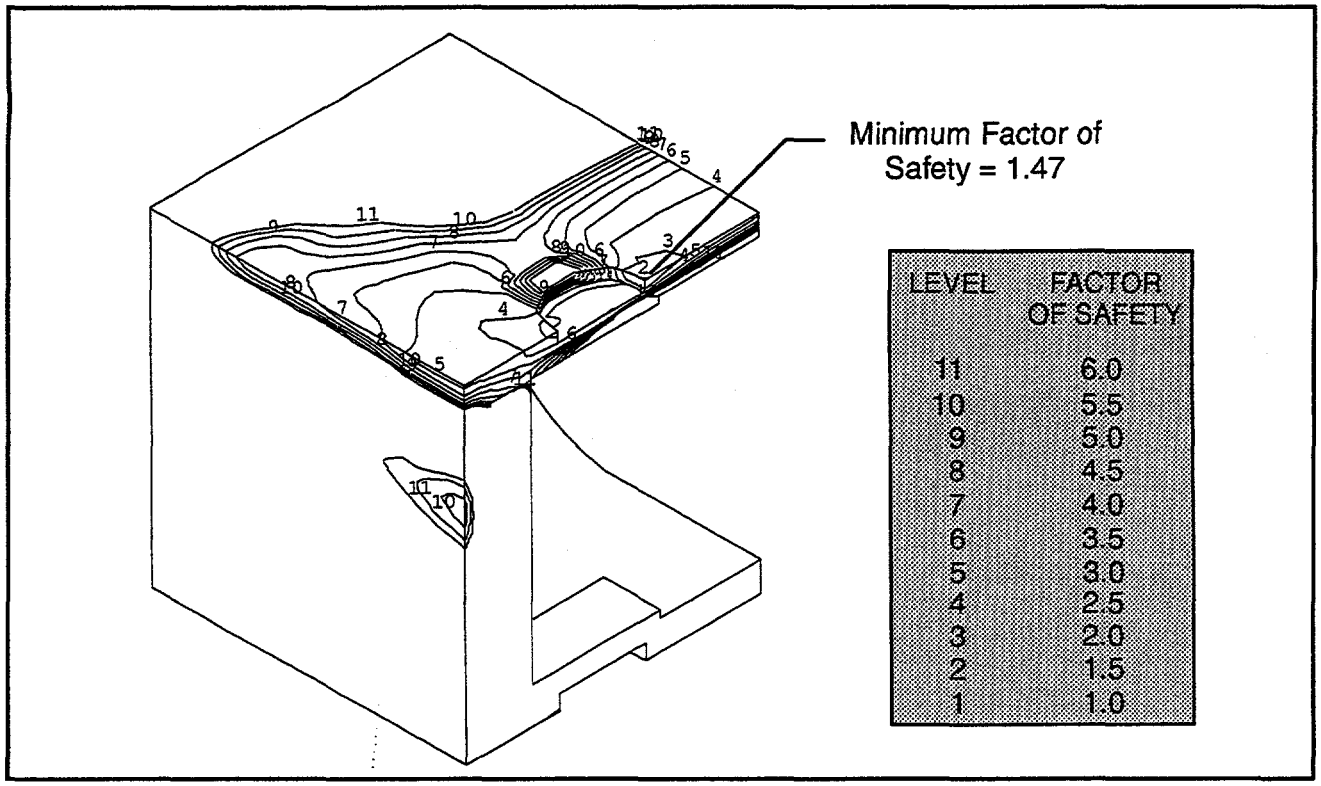

Figure 3-20. X Stress Factor of Safety Contours, T = 22 Sec, Alt = 189 kft Cassini GPHS Aeroshell, 7 Degree Face-On Stable Trajectory, No Roll

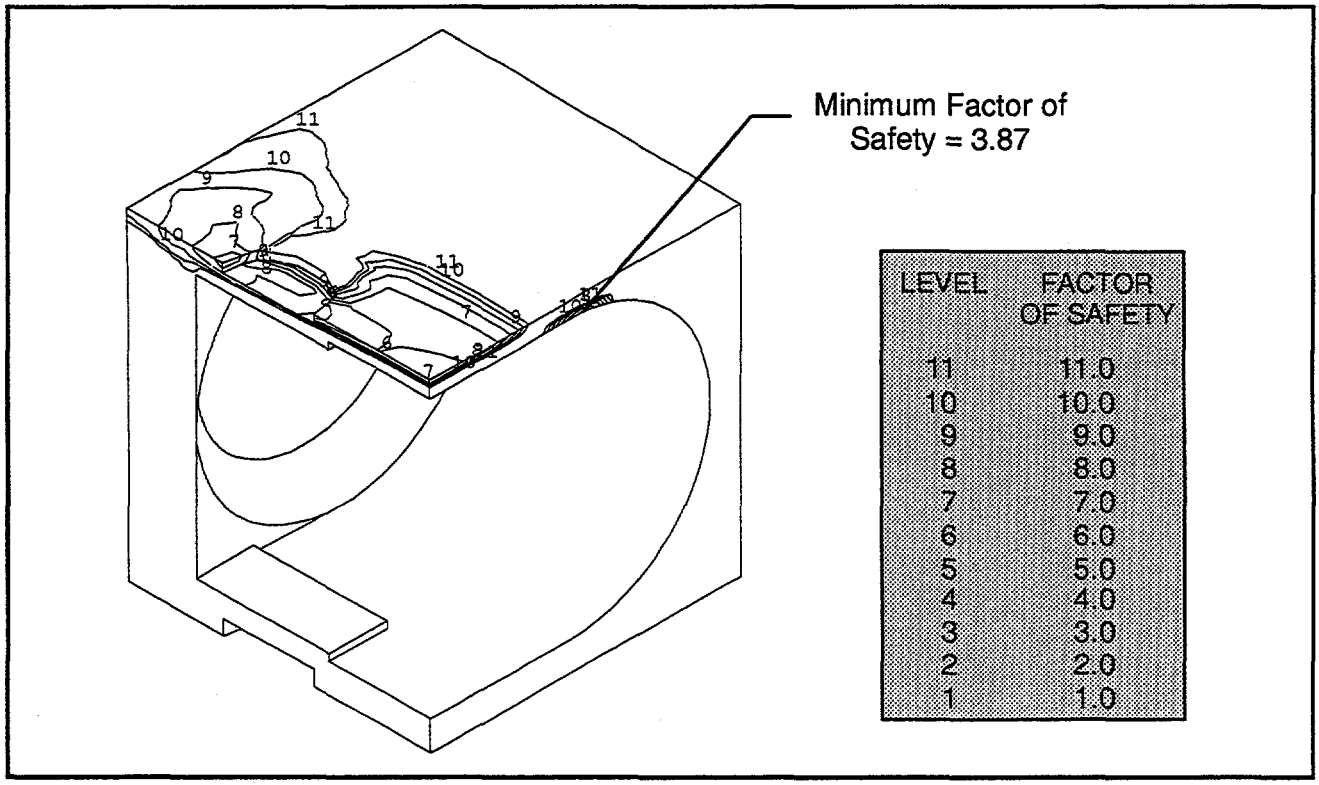

Figure 3-21. X Strain Factor of Safety Contours, T = 26 Sec, Alt = 176 kft Cassini GPHS Aeroshell, 7 Degree Face-On Stable Trajectory, No Roll

Consequence and Risk Analysis

Case 1.9 outputs (related to the Centaur explosion) from LASEP-T were analyzed with SPARRC to provide an early estimate range of consequence results. With the source terms consisting of seven different types of release, including ground release, fire ball effects, and air release, more than 800 SATRAP runs and 250 GEOTRAP runs were executed. For the variability of the weather conditions at KSC, a set of 128 days was used in the analysis. A shell script was written for the automation of code execution and file storage. Overall, highest exposure doses were found from workers and spectators which are the people closest to the launch site, and the main pathway is through inhalation. Lowest consequences were found to apply for days with off-shore winds, through seafood ingestion pathway. Results were presented and discussed at the INSRP review meeting on 17-19 January. This exercise has demonstrated the functionality of various code modules and corresponding databases.

The coding used to categorize the meteorological conditions at the launch site for October 1987-1991 was completed. A programming error that resulted in no wind reversal days was found and corrected. Category 2, which contains days that have offshore surface and offshore upper level winds during the midnight to 7 am launch window, but have a wind reversal at some axial plane during the 8 hours after the launch window, now contains 14 days. Category 3, grouping pure offshore days during the window and/or 8 hours after the window, now contains 7 days. Previous results had all of these days in category 3.

A preliminary investigation of the worker and spectator populations that might be available at KSC and CCAS was made. This investigation involved both the effects of having no on-site visitors, and the effects of nighttime and non-shuttle launch versus the currently available shuttle daytime worker and spectator population distributions. These preliminary results were provided to JPL for further investigation and clarification of visitor control policies to be employed for the launch. The current approach to this issue will be to apply factors to the available worker and spectator distributions. These factors will be treated in the uncertainty analysis.

Safety Test Program

The three converter test articles for the edge-on fragment test have been modified for mounting to the LANL support structure. Flange doublers and new mounting holes were added and new attachment hardware was provided. The converter test article for the hot engineering test was shipped to LANL this month. The remaining two test articles will be shipped early next month. Edge-on fragment testing is scheduled to be completed in February 1996.

TASK 4 QUALIFIED UNICOUPLE FABRICATION

The remaining efforts in Task 4 are associated with testing of 18 couple modules. Test temperatures and life test hours are shown in Table 4-1.

Table 4-1. Test Temperatures and Life Test Hours

Module	Unicouple Source	Test Temperature Hot Shoe	Status as of 28 January 1996
18-10	Early Qualification Lot	1135°C	10,400 hours Performance Normal Test Terminated October 1994
18-11	Full Qualification Lot	1135°C	16,872 Hours Performance Normal
18-12	Early Flight Production Lot	1035°C	12,690 Hours Performance Normal

18 Couple Module Testing

Two modules remain on life test. Testing of module 18-10 was terminated at the end of October 1994 after 10,400 hours.

Module 18-11 (1135°C)

On 28 January 1996, the module reached 16,872 hours at the accelerated hot shoe temperature of 1135°C. Measured performance during this period continues to fall within the data base established by MHW and GPHS 18 couple modules.

The thermoelectric performance evaluation primarily studies the trends of the internal resistance and power factor. Figures 4-1 and 4-2 show these trends in comparison to module 18-8, the last module built during the GPHS program. Agreement is excellent and provides a high degree of confidence that the GPHS unicouple manufacturing processes have been successfully replicated. Table 4-2 summarizes the initial and 16,872 hour performance data.

The isolation resistance trend between the thermoelectric circuit and the foil is shown in Figure 4-3 with modules from the MHW and GPHS programs. The isolation resistance plateaued at about 1000 ohms between 6,000 and 7,000 hours. It then started a slow decrease and is presently at 566 ohms. A similar plateau and gradual decline were observed in MHW module SN-1. At the accelerated temperature of 1135°C the same amount of sublimation occurs in about 1,650 hours of testing as would occur in a 16-year Cassini mission.

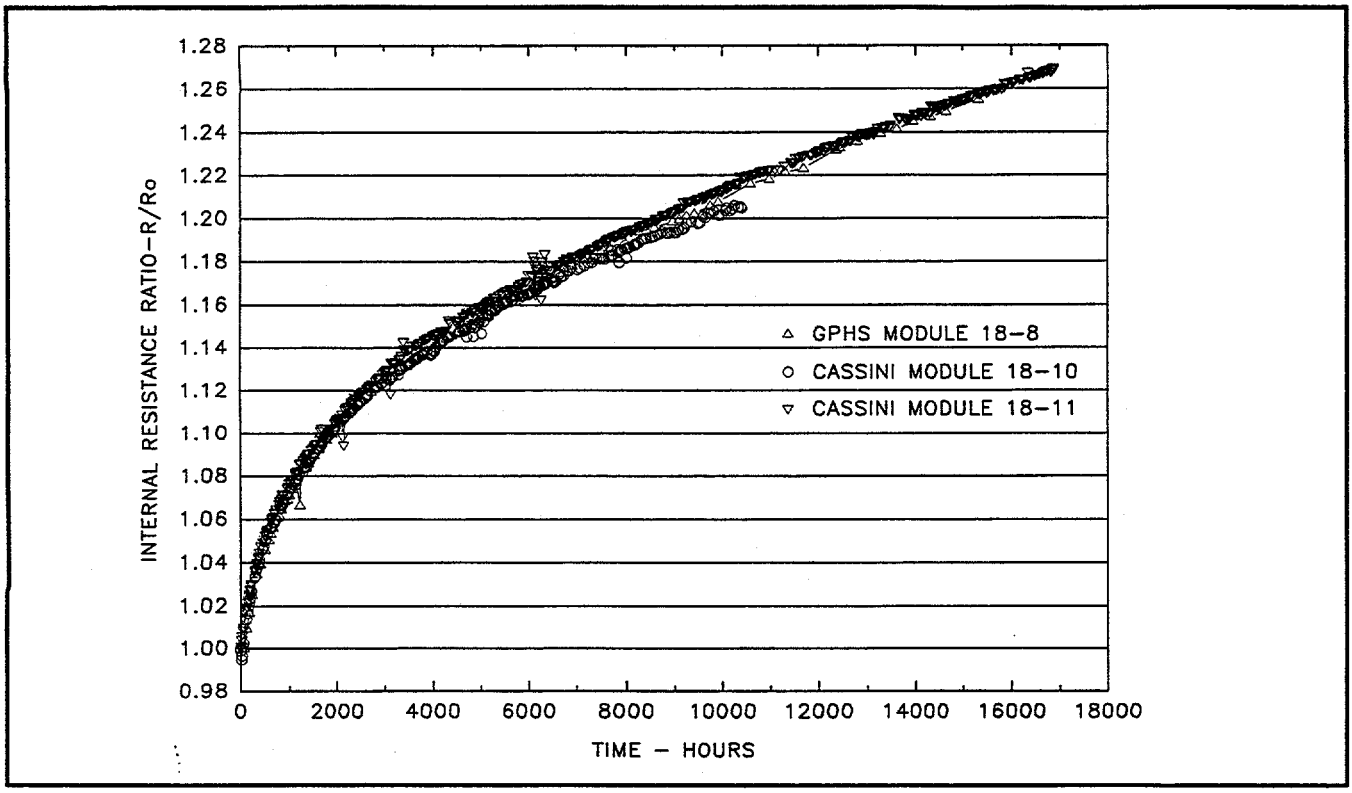

Figure 4-1. Internal Resistance Ratio Versus Time (Modules 18-10, 18-11, GPHS Module 18-8) – 1135°C Operation

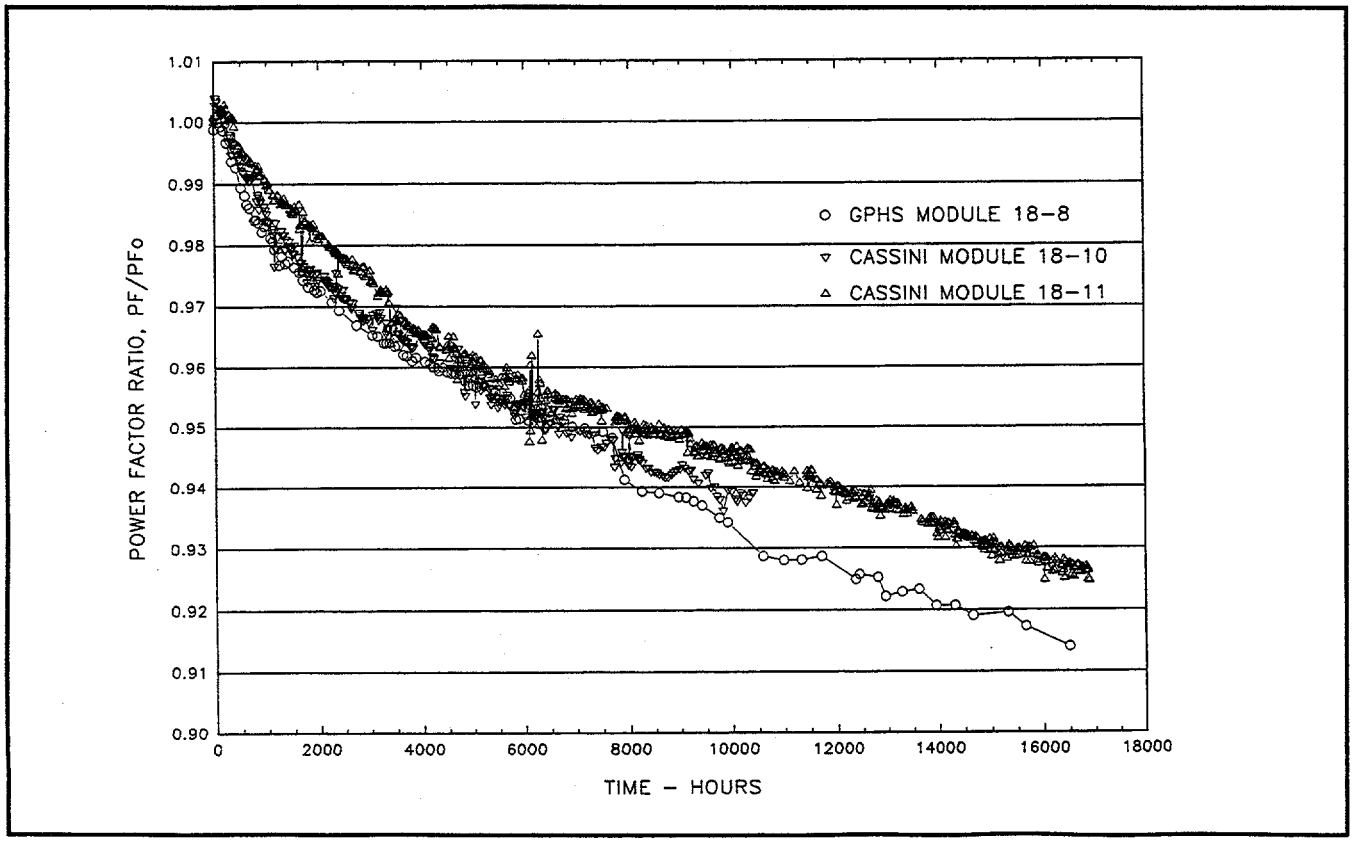

Figure 4-2. Power Factor Ratio Versus Time (Modules 18-10, 18-11, GPHS Module 18-8) – 1135°C Operation

Table 4-2. Comparison of Initial and 16,872 Hour Performance of Module 18-11 at 1135°C

	Initial 2/2/94	t = 52 hours V_L = 3.5V 2/4/94	t = 16,872 hours 1/28/96
Heat Input, Watts	190	192.9	192.8
Hot Shoe, °C Average	1137.8	1137.5	1107.7
Hot Shoe Range °C	5.4	5.2	9.0
Cold Strap, °C Average (8 T/Cs)	311.9	314.3	305.9
Cold Strap Range (8T/Cs)	2.6	2.5	2.1
Cold Strap Average (12 T/Cs)	306.5	308.9	300.9
Cold Strap Range (12 T/Cs)	20.1	20.3	18.9
Load Voltage, Volts	3.895	3.499	3.492
Link Voltage, Volts	0.108	0.121	0.097
Current, Amps	2.842	3.174	2.794
Open Circuit Voltage, Volts	7.140	7.160	7.505
Normalized Open Circuits (8T/Cs)	6.319	6.359	6.851
Normalized Open Circuits (12 T/Cs)	6.276	6.316	6.817
Average Couple Seebeck Coefficient (12)	498×10^{-6}	501×10^{-6}	540.2×10^{-6}
Internal Resistance, Ohms	1.104	1.115	1.402
Internal Resistance Per Couple (Avg.)	0.0613	0.0620	0.0776
Power Measured, Watts (Load + Link)	11.375	11.492	10.03
Power Normalized, Watts (8 T/Cs)	8.909	9.065	8.36
Power Normalized, Watts (12 T/Cs)	8.789	8.942	8.25
Power Factor	40.452×10^{-5}	40.557×10^{-5}	37.47×10^{-5}
Isolation			
Circuit to Foil, Volts	-1.68	-1.36	-1.65
Circuit to Foil, Ohms	6.29K	5.95K	0.57K

Consequently, approximately 10.2 times as much sublimation has occurred during the test duration of module 18-11 as will occur during the Cassini mission. The module performance, therefore, confirms the adequacy of the silicon nitride coating on the qualification couples.

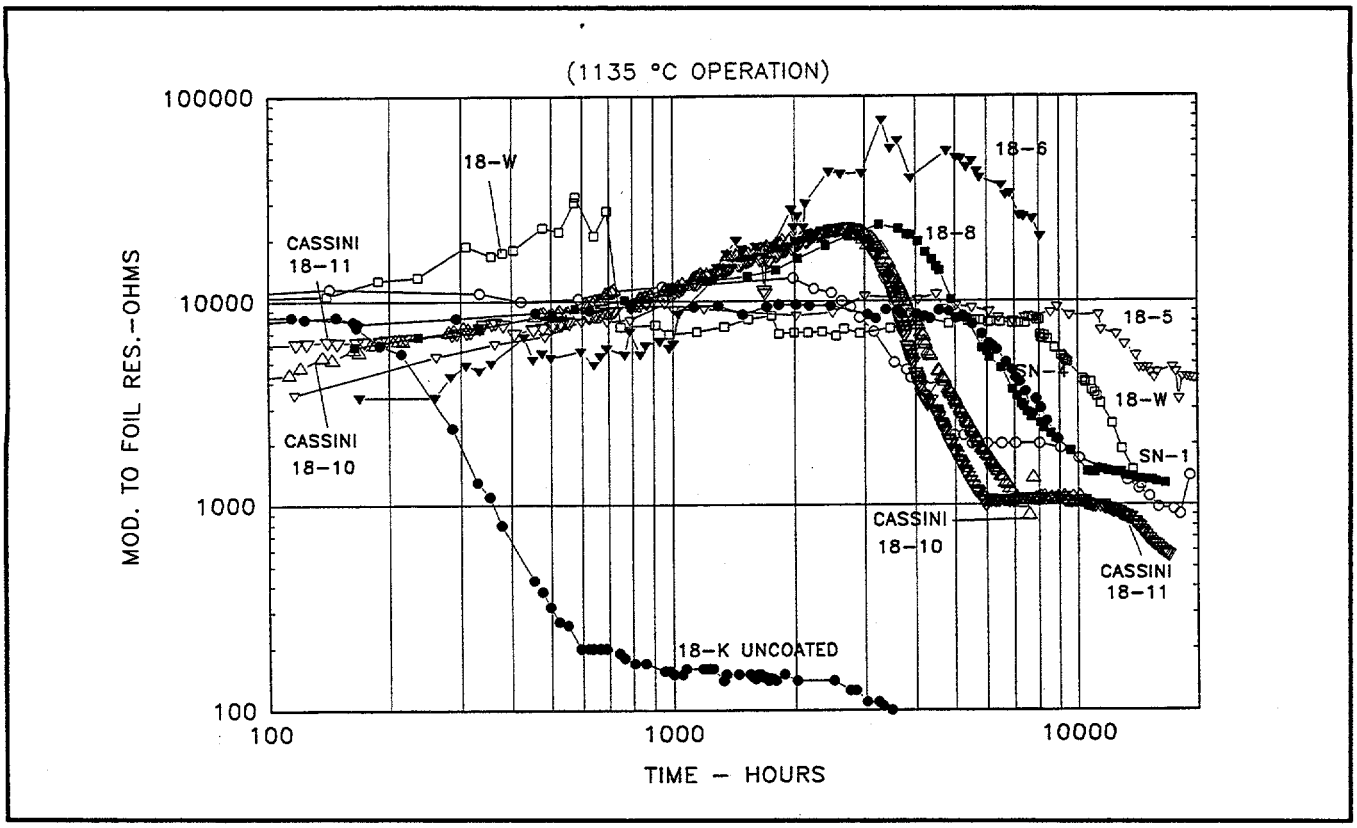

Figure 4-3. Isolation Resistance – Module Circuit to Foil (Modules 18-10, 18-11, GPHS Module 18-8) – 1135°C Operation

Individual Unicouple Performance:

The performance of individual unicouples and rows of unicouples continues to be observed. Table 4-3 shows the room temperature resistance changes and the internal resistance changes observed during operation for each of the six rows and for individual unicouples in Rows 2 and 5. The unicouples continue to perform within a narrow band.

Module 18-12 (1035°C Operation)

The module reached 12,690 hours at the normal operating temperature of 1035°C on 28 January 1996 . Thermoelectric performance, as measured by internal resistance and power factor trends, continues to be normal as shown as Figures 4-4 and 4-5, respectively. Table 4-4 shows initial performance and the performance on 28 January 1996.

Isolation Resistance

The isolation resistance between the circuit and foil continues to show the normal trend as shown in Figure 4-6.

Individual Unicouple Performance

A review of the unicouple internal resistances and open circuit voltages indicates that all unicouples are exhibiting very similar behavior with time (See Table 4-5). The data for the six individually instrumented unicouples in Rows 2 and 5 are shown in Figure 4-7.

Table 4-3. Module 18-11 Internal Resistance Changes

Position	Serial #	2nd Bond Milliohm	Preassy Milliohm	Delta ri Milliohm	T = 0 Milliohm	T=1,509 Hours	Delta ri Milliohm	Percent Increase	T=16,872 Hours	Delta ri Milliohm	Percent Increase
1.0	H2006	22.50	22.10	-0.40							
2.0	H0507	22.40	21.90	-0.50							
3.0	H0512	22.7	22.20	-0.50							
					182.30	199.70	17.40	9.54	232.5	50.20	27.50
4.0	H0439	23.20	22.70	-0.50	62.30	67.90	5.60	8.99	78.80	16.50	26.50
5.0	H0587	22.50	22.40	-0.10	61.00	66.50	5.50	9.02	76.90	15.90	26.10
6.0	H0657	22.70	22.50	-0.20	61.40	67.30	5.90	9.61	78.20	16.80	27.40
					184.10	201.10	17.00	9.23	233.10	49.00	26.60
7.0	H0585	22.90	22.50	-0.40							
8.0	H0459	22.50	22.10	-0.40							
9.0	H0562	22.70	22.30	-0.40							
					185.70	203.20	17.50	9.42	236.90	51.20	27.60
10.0	H0248	22.70	22.30	-0.40							
11.0	H0163	22.90	22.40	-0.50							
12.0	H0282	22.70	22.40	-0.30							
					184.90	201.70	16.80	9.09	233.10	48.20	26.10
13.0	H0428	23.10	22.70	-0.40	62.10	67.90	5.80	9.34	78.70	16.60	26.70
14.0	H0326	22.60	22.00	-0.60	62.20	68.30	6.10	9.81	79.70	17.50	28.10
15.0	H0232	22.60	22.00	-0.60	60.90	66.60	5.70	9.36	77.90	17.00	27.90
					184.70	202.30	17.60	9.53	235.60	50.90	27.60
16.0	H0590	22.60	22.40	-0.20							
17.0	H0393	22.60	22.10	-0.50							
18.0	H0496	22.50	22.30	-0.20							
					184.20	201.40	17.20	9.34	232.80	48.60	26.40

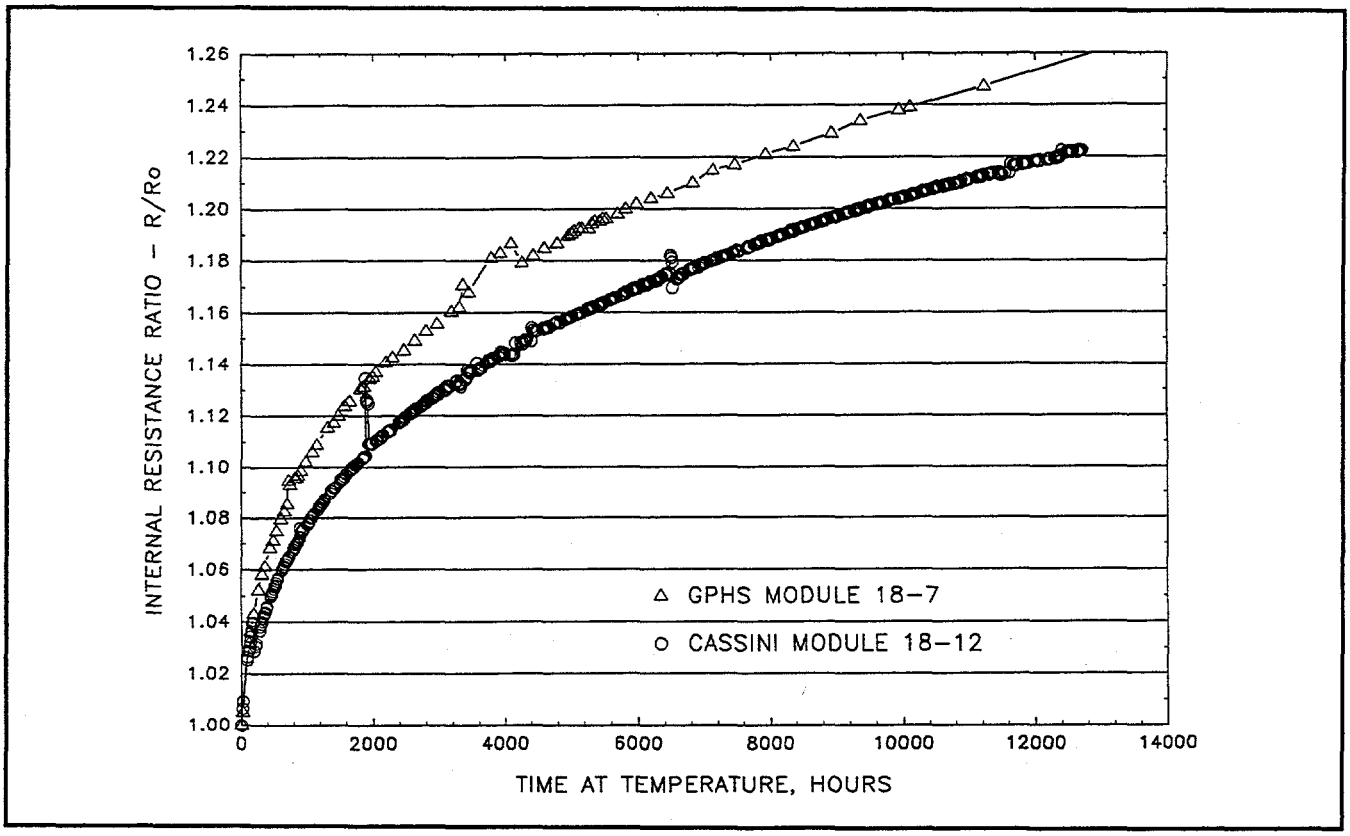

Figure 4-4. Internal Resistance Ratio Versus Time (Modules 18-12, and 18-7) – 1035°C Operation

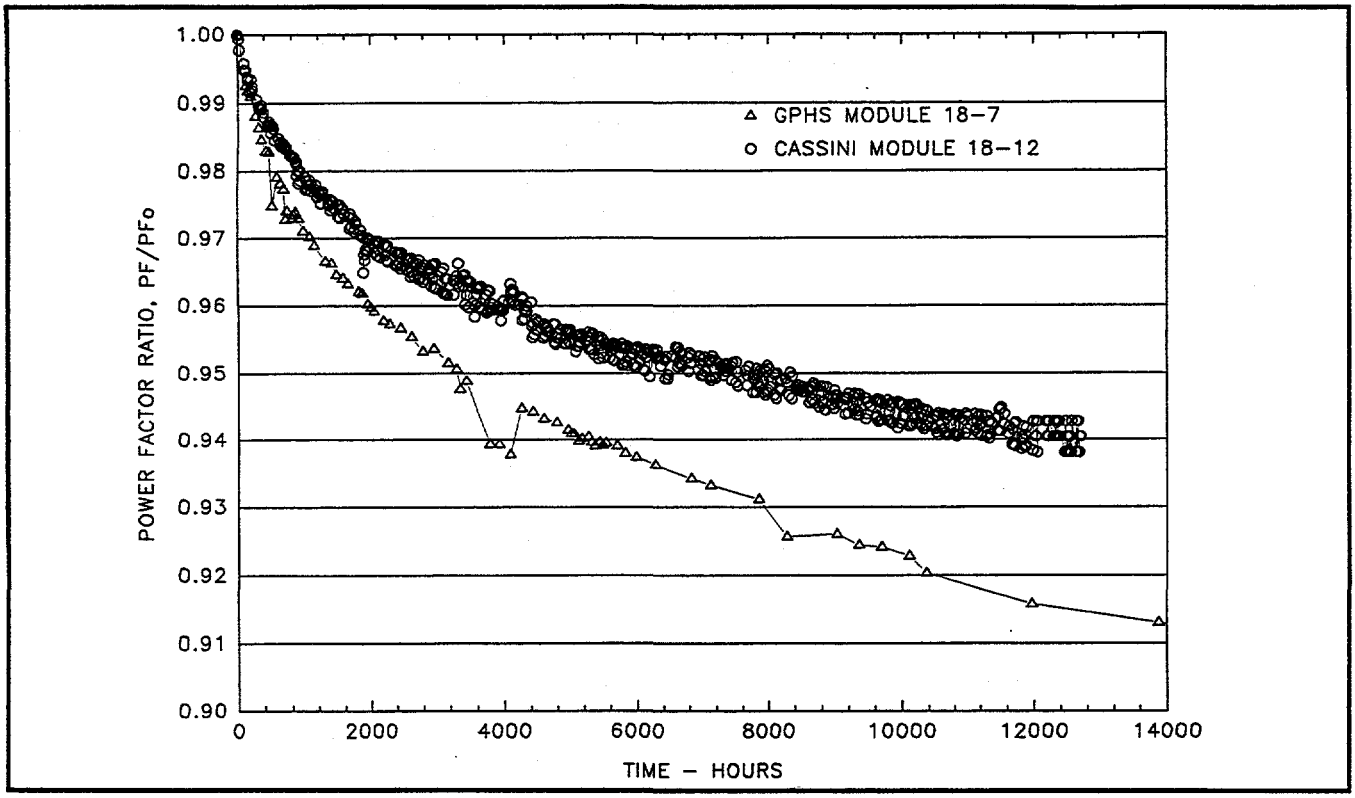

Figure 4-5. Power Factor Ratio Versus Time at Temperature (18-7 and 18-12) – 1035°C Operation

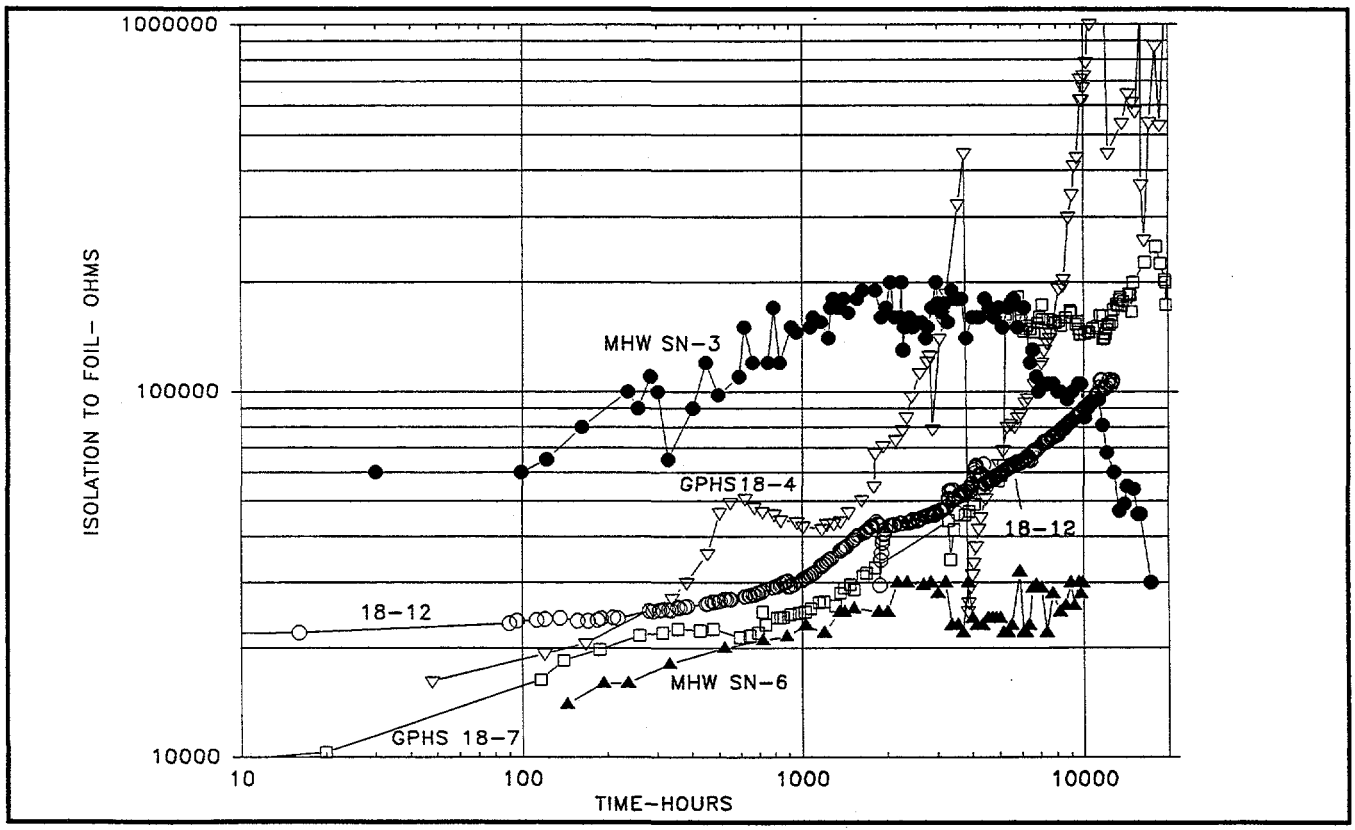

Figure 4-6. Isolation Resistance – Module Circuit to Foil (18-12, GPHS and MHW Modules) – 1035°C Operation

Table 4-4. Comparison of Initial and 12,690 Hour Performance of Module 18-12 at 1035°C

	Initial 6/16/94	t = 12,690 Hours 1/28/96
Heat Input, Watts	169.15	169.4
Hot Shoe, °C Average	1035.9	1028.5
Hot Shoe Range °C	5.7	3.6
Cold Strap, °C Average (8 T/Cs)	287.1	283.9
Cold Strap Range (8T/Cs)	5.0	5.4
Cold Strap Average (12 T/Cs)	282.7	279.5
Cold Strap Range (12 T/Cs)	19.8	19.5
Load Voltage, Volts	3.578	3.498
Link Voltage, Volts	0.155	0.154
Current, Amps	2.548	2.473
Open Circuit Voltage, Volts	6.431	6.854
Normalized Open Circuit (8T/Cs)	6.307	6.761
Normalized Open Circuit (12 T/Cs)	6.268	6.720
Average Couple Seebeck Coefficient (12)	497×10^{-6}	533.3×10^{-6}
Internal Resistance, Ohms	1.053	1.294
Internal Resistance Per Couple (Avg.)	0.0588	0.0719
Power Measured, Watts (Load + Link)	9.510	9.03
Power Normalized, Watts (8 T/Cs)	9.146	8.79
Power Normalized, Watts (12 T/Cs)	9.011	8.66
Power Factor	42.06×10^{-5}	39.55×10^{-5}
Isolation		
Circuit to Foil, Volts	-1.71	-0.851
Circuit to Foil, Ohms	21.3K	106.2K

Table 4-5. Module 18-12 Internal Resistance Changes

Position	Serial #	2nd Bond Milliohm	Preassy Milliohm	Delta ri Milliohm	T = 0 Milliohm	T=1,505 Hours	Delta ri Milliohm	Percent Increase	T=12,690 Hours	Delta ri Milliohm	Percent Increase
1.0	H2594	23.80	22.90	-0.90							
2.0	H2634	22.70	22.60	-0.10							
3.0	H2606	23.50	22.40	-1.10							
					176.80	192.10	15.30	8.65	213.9	37.10	21.00
4.0	H2168	22.20	21.70	-0.50	57.50	63.30	5.80	10.09	71.10	13.60	23.70
5.0	H2151	22.40	21.90	-0.50	57.40	62.90	5.50	9.58	70.40	13.00	22.60
6.0	H2256	22.20	21.70	-0.50	57.00	63.10	6.10	10.70	71.10	14.10	24.70
					171.20	188.60	17.40	10.16	211.90	40.70	23.80
7.0	H2597	24.40	23.20	-1.20							
8.0	H2680	22.60	23.00	0.40							
9.0	H2658	22.70	23.00	0.30							
					178.00	193.60	15.60	8.76	215.40	37.40	21.00
10.0	H1506	23.50	23.20	-0.30							
11.0	H1392	23.80	23.00	-0.80							
12.0	H1606	23.60	22.60	-1.00							
					176.20	193.40	17.20	9.76	216.10	39.90	22.60
13.0	H1344	23.60	23.50	-0.10	59.20	64.80	5.60	9.46	72.30	13.10	22.10
14.0	H1618	23.30	24.00	0.70	58.60	64.50	5.90	10.07	72.30	13.70	23.40
15.0	H1262	23.70	23.30	-0.40	59.40	65.00	5.60	9.43	72.60	13.20	22.20
					176.60	193.70	17.10	9.68	216.60	40.00	22.70
16.0	H1580	23.00	23.70	0.70							
17.0	H2127	22.80	22.10	-0.70							
18.0	H2113	22.90	22.20	-0.70							
					174.50	191.30	16.80	9.63	214.00	39.50	22.60

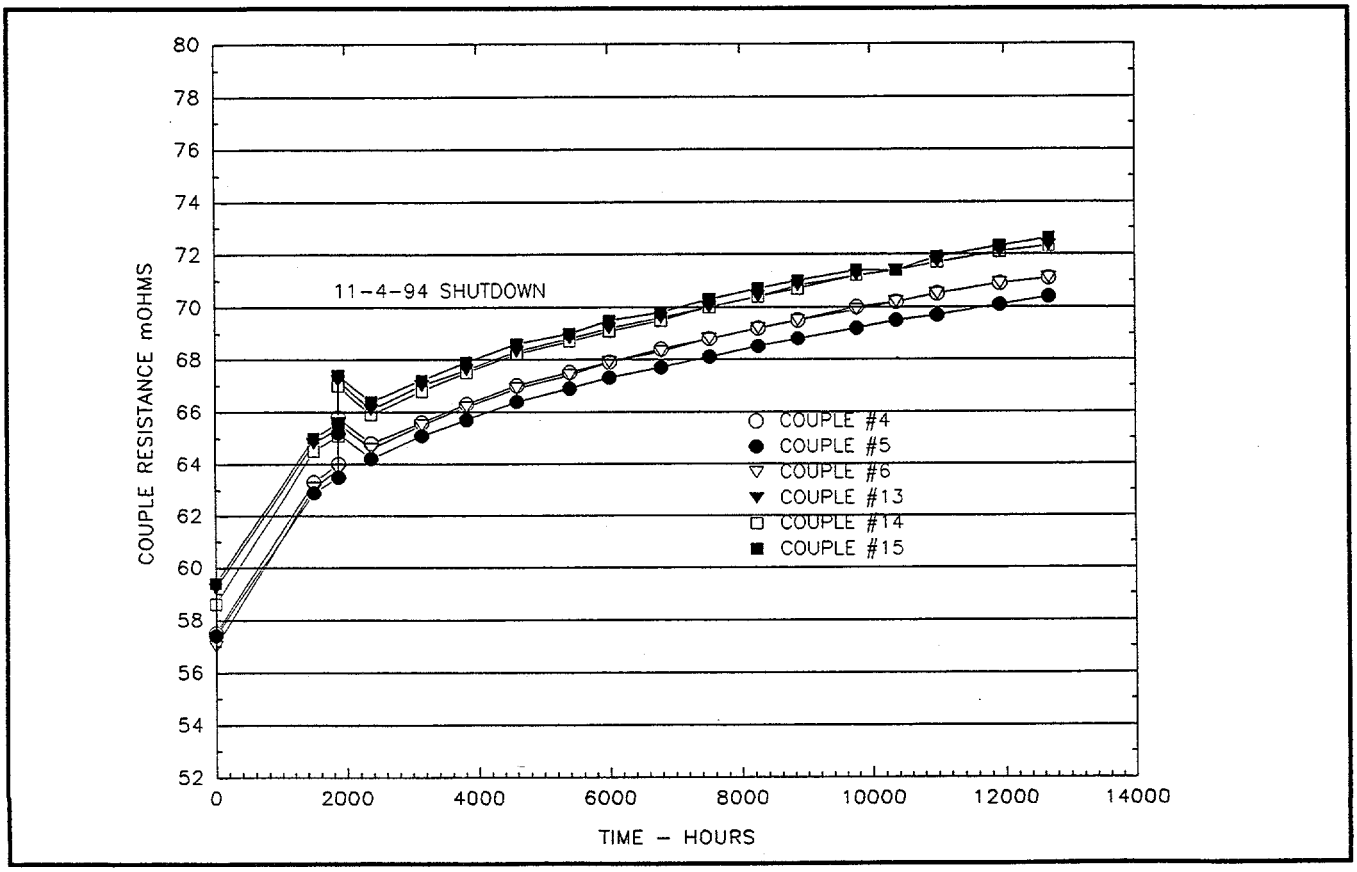

Figure 4-7. Individual Unicouple Internal Resistance Trends (Module 18-12)

TASK 5 ETG FABRICATION, ASSEMBLY, AND TEST

E-6 ETG Test Activity (Building 800)

The E-6 ETG continues in storage in Building 800. ETG and CSC pressures are being monitored and adjusted, as required, to maintain storage pressure requirements.

E-7 ETG Rework Activity

ETG rework was completed on 4 January, and the ETG was installed into the shipping container and delivered to Building 800 on 5 January. This completed the rework of E-7 approximately ten weeks ahead of the originally scheduled date.

E-7 Processing and Testing

On 9 January, the converter shipping container was opened, and the ETG was removed and installed on the transfer cart. ETG resistance measurements were completed and the data obtained compared favorably with resistance data obtained in Building B.

After installation of the power cable and connection of the pneumatic lines, the ETG was installed in LAS-2. GSE cables were connected and the ROC checkout was completed successfully. The ETG was vented and the outboard dome and midspan caps were removed in preparation for processing.

On 11 January, a Segment Readiness Review was held (chaired by the Cassini Product Assurance Manager) and approval was granted for test start-up.

The LAS was evacuated and EHS heating was initiated on 13 January. Normal heat-up continued until 15 January when a partial argon gas backfill of the LAS occurred. After verifying the integrity of the system, the LAS was re-evacuated. The backfill may have been caused by electronic noise. A recorder was installed to monitor the voltage of the cathode gage circuit that controls the backfill system. Also, a time delay was installed in this circuit to prevent voltage spikes from initiating backfill.

E-7 Processing and Testing (Cont'd)

EHS heat inputs continued and on 27 January, the ETG open circuit voltage reached 35 volts. At this time, EHS power inputs were suspended while the load voltage was adjusted from 18.5 to 30 volts in increments so as not to exceed the ETG partial pressure requirements. On 28 January, normal power increases were resumed and the EHS power input was approximately 3200 watts. The ETG performance is normal and consistent with previous ETGs at this heat Input.

E-8 Converter Hardware

Rework of the EHS heater leads was initiated. This requires removal of the existing leads and replacing them with new leads. This was necessary in order to eliminate nylon contamination which occurred after welding. The graphitic components were also baked out to eliminate possible residual nylon contamination. The re-assembly and welding of the new leads will be performed during the next reporting period.

The shell and fin assembly was painted with PD 224 high emissivity paint and the air curing process was completed. Following application of the boron nitride coating in the C-seal surface, the assembly will be sent to an outside vendor for the final vacuum curing process.

TASK 6 GROUND SUPPORT EQUIPMENT (GSE)

Dye penetrant inspection was completed on the five welded RTG shipping cage extensions. Proof loading of the RTG shipping container base and cage to be used for the Trailblazer activity was successfully completed. The ETG lifting sling was also proof loaded.

Machining of the brackets for the first of three converter support ring assemblies continued. The first set is expected to be completed in February. The second two sets of brackets will be completed in the second quarter.

TASK 7 RTG SHIPPING AND LAUNCH SUPPORT

Launch Activity

A revised set of RTG related Trailblazer procedures were received from JPL and are being reviewed. Modification of the shipping container to be used for Trailblazer was completed.

TASK 8 DESIGNS, REVIEWS, AND MISSION APPLICATIONS

8.1 Galileo/Ulysses Flight Performance Analysis

No significant activity this reporting period.

8.2 Individual and Module Multicouple Testing

This task has been successfully completed.

8.3 Structural Characterization of Candidate Improved N- and P-Type SiGe Thermoelectric Materials

This task has been successfully completed.

8.4 Technical Conference Support

No significant activity this reporting period

8.5 Evaluation of an Improved Performance Unicouple

Module 18-Z

This task has been successfully completed.

8.6 Solid Rivet Feasibility Study

This task has been successfully completed.

8.7 Computational Fluid Dynamics (CFD)

Work continues on the CFD task. Because this task is closely related to the Task 3 safety activities, technical progress is reported under that task.

8.8 Technical International Conference Support

This task has been successfully completed.

8.9 Additional Safety Tasks

Additional safety efforts have been assigned to this task. Because these efforts are closely related to the Task 3 safety activities, technical progress is being reported under that task.

TASK 9 PROJECT MANAGEMENT, QUALITY ASSURANCE, AND RELIABILITY

9.1 Project Management

Task 9.1 Project Management

On 11 January the Cassini RTG Program celebrated its 5th anniversary. During this five year period all contractual reports, CDRLs, and milestone documents were delivered on schedule.

The rework on E-7 was completed approximately ten weeks ahead of schedule and the ETG was shipped to Building 800 for processing the first week of January. Processing began the second week of January and is continuing satisfactorily with the EHS power input at 3200 watts as of the end of this reporting period.

Support was provided for the E-2 Readiness Review at Mound and Lockheed Martin personnel installed the RTD cable and PRD mounting plate prior to E-2 fueling. Support also was provided for the following safety working group reviews and meetings: INSRP at LMMS in Valley Forge, and Fireball Modeling at Sandia Labs, NM.

Technical papers were presented at the Space Technology and Applications International Forum in Albuquerque, NM.

Attached is the Cassini RTG program calendar for 1Q96 showing program meetings and important related events.

No significant environmental, health, or safety incidents occurred during this period.

9.2 Quality Assurance

Quality Plans and Documents

No plans were initiated or modified during this period.

Quality Control in Support of Fabrication

E-7 Converter: Rework of the E-7 converter was completed during the first week of this reporting period. It was then placed in the shipping container and transported to Building 800 for processing and acceptance testing. The Test Readiness Review was successfully conducted and approval was granted to commence processing. Thus far, all parameters are nominal and processing is continuing.

E-8 Converter: Work on subassemblies for E-8 is continuing. E-8 hardware is being assembled into kits so that it could be fully assembled at some point in the future, if required. In-process inspection support has been provided during assembly of the EHS as well as for the PD 224 and boron nitride painting operations. No significant problems have been noted with E-8 hardware.

Unicouple Production

Effort to upgrade specifications and drawings to accurately describe all processes for future builds has been completed.

E-6 Converter

The E-6 converter remains in the shipping container and is in long term storage in Building 800 until required for processing at Mound. Internal pressure is being monitored on a regular basis and gas is being replenished, as required. The ETG C of I has been reviewed and was re-submitted for removal of many of the conditional approvals.

Quality Assurance Audits

There was no audit activity during this reporting period.

Quality Assurance Status Meeting

No general status meetings were held during this reporting period.

TASK H CONTRACTOR ACQUIRED GOVERNMENT OWNED (CAGO) PROPERTY ACQUISITION

Task H.1 CAGO Unicouple Equipment

No significant activity during this reporting period.

H.2 CAGO - ETG Equipment

No significant activity during this reporting period.

H.3 CAGO - MIS

No significant activity during this reporting period.

H.4 CAGO (Building 800)

No significant activity during this reporting period.

Cassini RTG Program Calendar

As of 21 February 1996

1st QTR 1996

	M	T	W	T	F	S	S	FW
JANUARY	1 Happy New Year 	2 F-2 Paint and Modifications - EG&G Mound - *Reinstrom, et al*	3	4 Fireball Model Sandia National Labs (Albuquerque) *Braun, Chang, DeFillipo*	5	6	7	01
	8	9 Space Technology and Applications International Forum - Albuquerque, New Mexico - Josloff	10	11 *Cassini 5th Anniversary* F-2 Readiness Review - EG&G Mound - *Cockfield, Reinstrom*	12	13	14	02
	15	16	17 INSRP Review - Sheraton Hotel - Valley Forge - *Braun, et al*	18	19	20	21	03
	22	23 Monthly Reports Due to DOE	24	25 F-2 Support - EG&G Mound - *Kugler*	26	27	28	04
FEBRUARY	29	30 Cassini Quarterly Program Review OSC, Germantown MD - *Hemler, Cockfield, Reinstrom, DeFillipo*	31	1	2 F-2 Support - EG&G Mound - *Cockfield*	3	4	05
	5 F-2 Support - EG&G Mound - *Cockfield*	6 Safety Test Hot Eng. Fragment Test - Albuquerque, New Mexico - *Hartman, Kauffman*	7	8	9	10	11	06
	12 F-2 Support - EG&G Mound - *Kugler*	13	14 INSRP RESP Subpanel Review - El Segundo, CA - *Hemler/Cockfield/ DeFillipo/Tobery/Dayuitt/Letts/Vacek*	15 RTG Installation Cart Demo - JPL - CA - *Reinstrom/Cockfield*	16 F-2 Support - EG&G Mound - *Kugler*	17	18	07
	19	20	21 Operations Analysis On-Site Visit - EG&G Mound - *Reinstrom*	22	23 Monthly Reports Due to DOE	24	25	08
MARCH	26	27	28 Side-On Fragment Safety Test (TA-1) - Albuquerque, NM - *Hartman/Cockfield*	29	1 Sterling Franks Visit to Bldg. B - Valley Forge, PA - *Hinners/Hemler/et al*	2	3	09
	4	5	6	7	8	9	10	10
	11	12	13	14	15	16	17	11
	18 Trailblazer Test Readiness Review - Cape Canaveral, FL - *Haley/Reinstrom*	19	20	21	22 Monthly Reports Due to DOE	23	24	12
	25	26	27	28	29	30	31	13

Cassini RTG Program
Technical Report Distribution

BANNAN, K.M.	Space Power Library (2)
BRANDT, D.	U4019 Bldg. 100
BURGER, C.F.	20B41 Bldg. B
CENTURIONI, D.	Mezz Bldg. B
COCKFIELD, R. D.	20B41 Bldg. B
COLE, D.	M4018 Bldg. 100
CURRAN, J.	Mezz Bldg. B
DADD, S.	Mezz Bldg. B
DAYWITT, J.	U4019 Bldg. 100
DEANE, N.	San Jose Office
DE FILLIPO, L.E.	29B12 Bldg. B
DICKINSON, K.	29B12 Bldg. B
DOUGLAS, L.	Mezz Bldg. B
DOWER, A. G.	U7035 Bldg. 100
FRANKLIN, B.	Mezz Bldg. B
GRIMLEY, B.	Mezz Bldg. B
HALEY, V.F.	29B12 Bldg. B
HARTMAN, R.F.	29B12 Bldg. B
HEMLER, R.J.	29B12 Bldg. B
KAIN, S.A.	29B12 Bldg. B
KAMPAS, F.	20B41 Bldg. B
KAUFFMAN, R.	20B41 Bldg. B
KELLY, E.	20B41 Bldg. B
KLEE, P.M.	20B41 Bldg. B
KLINE, T.F.	29B12 Bldg. B
KUGLER, W.	20B41 Bldg. B
LETTS, B.	U7026 Bldg. 100
MONTGOMERY, J. L.	29B12 Bldg. B
MORGAN, E. M.	U3040 Bldg. 100
MORGAN, R. E.	29B12 Bldg. B
MURRAY, M.	29B12 Bldg. B
NAKAHARA, J.	29B12 Bldg. B
NYCE, R.	Mezz Bldg. B
REINSTROM, R.M.	29B12 Bldg. B
ROSKO, R.	20B41 Bldg. B
SAYDAH, A.R.	29B12 Bldg. B
SERENI, M.	Mezz Bldg. B
TOBERY, W.	20B41 Bldg. B
VICENTE, F.A.	29B12 Bldg. B
VIJAIYAN, K.	(FAX) DOE Canoga Park, CA
VACEK, D.	U4205 Bldg. 100
WAKS, J. M.	29B12 Bldg. B
ZULA, G.C.	29B12 Bldg. B

Inform Sally Kain X1597 of any changes, additions, or deletions.